p21-Senescent Cells Drive Pancreatic Islet Dysfunction Through Targetable Paracrine Signaling in Type 2 Diabetes

Kanako Iwasaki[1+], Priscila Carapeto[1+], Cristian Abarca[1], Francesko Hela[1], Stephanie Sanjines[1], Sebastian Peña[1], Sandra Le[1], Hui Pan[1], Maya Jackson[1], Christopher Cahill[1], Ayush Midha[1], Juliana Alcoforado Diniz[2], Dylan Baker[2], Sergii Domanskyi[2], Sara Espinoza[3], Alejandro Pena[4], Francisco G. Cigarroa[4], Jillian L. Woolworth[4], Jeffrey H. Chuang[2,5], Vesna D Garovic[6], James L. Kirkland[7], Tamar Tchkonia[7], Nicolas Musi[3], George A. Kuchel[8], Paul Robson[2], Cristina Aguayo-Mazzucato[1*]

+These authors contributed equally to this work

1. Joslin Diabetes Center/Harvard Medical School. Boston, MA
2. The Jackson Laboratory for Genomic Medicine, Farmington, CT
3. Center for Translational Geroscience, Department of Medicine, Cedars-Sinai Medical Center, Los Angeles, CA
4. UT Health San Antonio Transplant Center, San Antonio, TX
5. Department of Genetics and Genome Sciences, UConn Health, Farmington, CT
6. Division of Nephrology and Hypertension, Department of Medicine, Mayo Clinic, Rochester, MN
7. Center for Advanced Gerotherapeutics, Department of Medicine, Cedars-Sinai Medical Center, Los Angels, CA
8. UConn Center on Aging, UConn Health, Farmington, CT

*Corresponding author: cristina.aguayo-mazzucato@joslin.harvard.edu
Cristina Aguayo-Mazzucato MD PhD
Joslin Diabetes Center
Center for Life Sciences 5th floor
3 Blackfan Street, Boston, MA, 02215

ABSTRACT

Cellular senescence is an irreversible stress response, which leads to loss of cellular function and remodelling of the cellular secretory profile. In humans, pancreatic β-cells undergo cellular senescence during the progression to type 2 diabetes (T2D). However, the mechanism linking β-cell senescence to islet dysfunction remains unknown and thus, the therapeutic potential of targeting senescent cells in T2D is not established. Herein, we identified a subpopulation of senescent β-cells expressing p21, which emerged early in the progression of T2D in humans and mice. Spatial transcriptomics, and proteomics analyses confirmed senescence and loss of cellular identity in this subpopulation in humans. Functional analysis revealed lack of glucose responsiveness, high basal insulin secretion, and transcription of senescence-associated secretory phenotype (SASP) factors. SASP factors from $p21^+$ β-cells induced secondary senescence in neighbouring cells, characterized by dysfunction and loss of identity. Janus kinase inhibitors (JAKi) counteracted the induction of secondary senescence and restored β-cell function in islets from humans with T2D and in high-fat diet-fed mice. These findings reveal the critical role of $p21^+$ β-cells in T2D pathogenesis and the therapeutic potential of targeting this pathophysiological process.

GRAPHICAL ABSTRACT

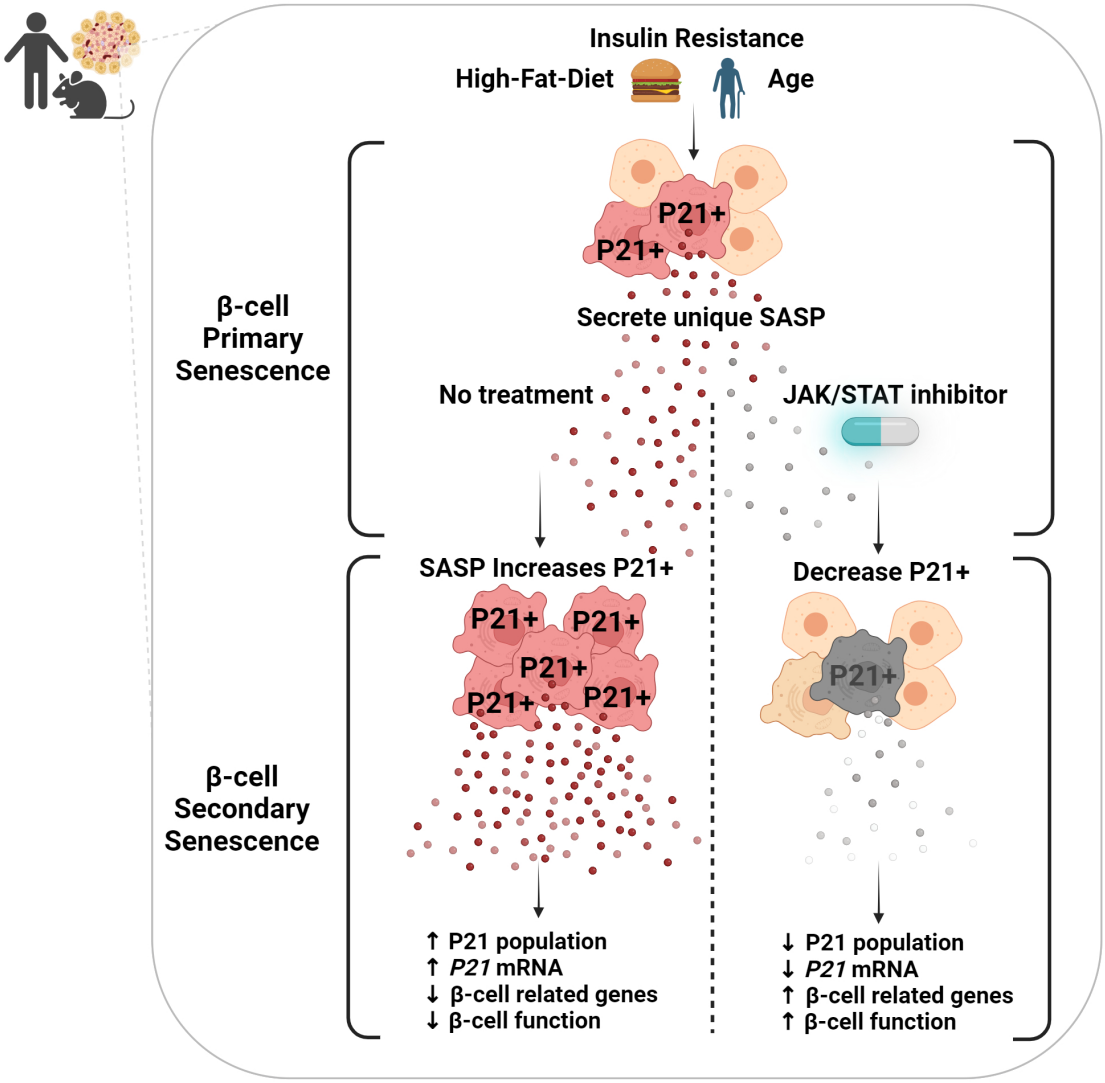

INTRODUCTION

As cells age or experience stress, they can enter a state of cellular senescence characterized by stable cell-cycle arrest, cellular dysfunction, resistance to apoptosis, and continued metabolic activity accompanied by secretion of senescence-associated secretory phenotype (SASP) factors. Beyond cell-autonomous effects, the SASP can induce secondary senescence in neighboring cells, thereby amplifying tissue dysfunction (1) and driving age-related diseases.

Insulin resistance and type 2 diabetes (T2D) are associated with increased senescence markers in mouse and human pancreatic β-cells (5, 6). Senescent β-cells are dysfunctional and a secrete a distinct SASP enriched in inflammatory and extracellular matrix remodeling factors (6–9). In mouse models, senolytic interventions improved insulin sensitivity, glucose homeostasis, and β-cell identity and function while reducing SASP gene expression (6, 10). However, whether β-cell SASP factors propagate secondary senescence within pancreatic islets remains unknown. An alternative strategy to targeting senescent β-cells is suppression of the SASP itself.

Notably, β-cell senescence may not be uniformly detrimental. Some studies suggest senescence-associated programs can promote immune surveillance, cell survival, differentiation, and insulin secretion (14, 15). These apparently conflicting observations may reflect underlying heterogeneity among senescent β-cells, consistent with the heterogeneous distribution of senescence markers within pancreatic islets (5). However, the identity, functional properties, and non-cell autonomous effects of distinct senescent β-cell populations remain poorly understood. Defining this heterogeneity will be essential

for developing effective and safe therapeutic approaches for chronic diseases associated with β-cell senescence, including T2D.

The cyclin-dependent kinase inhibitors p21 and p16 are major mediators of senescence across multiple cell types. These pathways, encoded by *Cdkn1a* and the *Cdkn2a* locus, respectively, are activated by diverse stressors including oncogene activation, telomere shortening, DNA damage, protein aggregation, and reactive oxygen species (ROS) (2).

Herein, senescent β-cell heterogeneity is hypothesized to be driven by differential activation of the cell-cycle arrest pathways mediated by *Cdkn1a* (p21) and *Cdkn2a* (p16). We identified distinct senescent β-cell subpopulations based on expression of these cell-cycle inhibitors. In C57BL/6 mice, *Cdkn1a*-expressing β-cells represented the predominant senescent population and were characterized by canonical SASP activation, impaired β-cell function, and loss of β-cell identity. Spatial transcriptomic and proteomic analyses of human pancreas tissue revealed that *CDKN1A*/p21+ INS+ cells downregulated key β-cell genes and transcription factors. Factors secreted by *Cdkn1a*+ β-cells induced secondary senescence in neighboring islet cells, leading to impaired glucose-stimulated insulin secretion and loss of β-cell identity. JAK1/2 inhibition prevented SASP-mediated secondary senescence and restored β-cell function. In human islets from donors with and without T2D, JAK1/2 inhibitors reduced p21 expression, suppressed SASP secretion, and improved glucose responsiveness. Together, these findings identify senescent β-cell heterogeneity as a critical determinant of islet dysfunction and demonstrate that specific targeting of SASP signaling mitigates secondary senescence and restores β-cell function in both mice and humans.

RESULTS

p21$^+$ senescent β-cells in mice are dysfunctional and lose transcriptional identity

We used previously published scRNASeq data (1) to analyze gene expression in pancreatic islets from 6- to 9-month-old male mice following acute induction of insulin resistance with the insulin receptor antagonist S961, with and without a two-week recovery period (**Fig. 1A**) completely reversing hyperglycemia and hyperinsulinemia (**Suppl. Fig. 1A**). β-cells, identified by the expression of *Ins2*, represented 64% of the total islet population in the control group (**Fig. 1B**). Other islet cell types were represented in the following proportions: α-11%, δ-9% PP-2%, ductal-2%, and endothelial-5% (**Suppl. Fig. 2**). Density estimates for the expression of *p21* (encoded by *Cdkn1a*) or *p16* (encoded by *Cdkn2a*) using a Gaussian finite mixture model identified at least two subpopulations of senescent β-cells: *Cdkn1a*$^+$ and *Cdkn2a*$^+$, as well as a third non-senescent of double-negative *Cdkn1a*$^-$/*Cdkn2a*$^-$ cells. Non-senescent (*Cdkn1a*$^-$/*Cdkn2a*$^-$) β-cells represented 75% of the total population of control islets. The remaining senescent cell subpopulations included 29% *Cdkn1a*$^+$ cells and 0.3% *Cdkn2a*$^+$ cells (**Suppl. Fig. 3**). These proportions align with reported values of 20-40% of *CDKN1A*$^+$ β-cells from adults over 60 years old (2). The frequency of the senescent subpopulation in other islet cell types is shown in **Suppl. Table 1**.

To determine whether the upregulation of *Cdkn1a* and *Cdkn2a* represented true senescence identities, co-expression with other senescence markers in the various subpopulations was evaluated (**Fig. 1C**). The *Cdkn1a*$^+$ subpopulation co-expressed cell proliferation regulator, *Jun* and the SASP factors *Il6* and *Il1b* while the *Cdkn2a*$^+$

subpopulation co-expressed *Glb1,* which encodes senescence marker β-galactosidase, and senescence marker *Hmgb1*. These results support the notion that these two subpopulations are in a state of senescence and are distinct from each other.

With insulin resistance, both the *Cdkn1a*$^+$ and *Cdkn2a*$^+$ senescent β-cell subpopulations increased (**Suppl. Fig. 3**). The *Cdkn1a*$^+$ subpopulation decreased during recovery, while the number of *Cdkn2a*$^+$ cells continued to increase (**Suppl. Fig. 3**), indicating distinct dynamics and discrete populations. Principal Component Analysis (PCA) of the z-scores revealed significant clustering by treatment (**Suppl. Fig. 4**); therefore, results are shown for all three treatments in each senescent subpopulation. Trajectory analysis of scRNASeq from non-senescent to senescent mouse β-cells revealed 5 stages based on transcriptional similarity, three of which appear to be alternate senescence fates, which we have named Stages 3A, B, and C, with stages 1 and 2 being non-senescent (**Fig. 1D)**. Characteristically, in β-cells from all metabolic conditions, Stage 3A had the highest *Cdkn1a* levels, Stage 3B was characterized by *Cdkn2a* expression while Stage 3C had high *Trp53* levels, suggesting a stressed cell fate. (**Fig. 1E**). *Cdkn1a*$^+$ β-cells in all metabolic conditions, had downregulated expression of hallmark β-cell genes, including *Ins1, Ins2, and Pdx1*, as well as functional genes under all metabolic conditions (**Fig. 1F, G, Suppl. Fig. 5A**). Interestingly, this set of functional genes was not downregulated in senescent *Cdkn2a*$^+$ β-cells (**Fig. 1F, G, Suppl. Fig. 5A**), revealing potential functional differences between subpopulations of senescent β-cells and reconciling previous reports of increased functionality after *p16* (*Cdkn2a*) overexpression in β-cells (3). Distinct *Cdkn1a*$^+$ and *Cdkn2a*$^+$ subpopulations have also been identified in other tissues, including adipose tissue, liver, and heart (4).

Expression of SASP factors in different senescent subpopulations included genes published in the SenMayo panel (5). To minimize artifacts introduced by specific gene dropout, only genes with quantifiable reads in all three subpopulations were included in the analysis and reported as β-SenMayo (**Fig. 1H, I , Suppl. Fig. 5B**). Compared with non-senescent and *Cdkn2a*$^{+}$ cells*, the Cdkn1a*$^{+}$ subpopulation had a significantly higher β-SenMayo score with increased transcripts of *Il1b*, *Plaur*, *Gdf15* and *Fgf1* (**Fig. 1I, Suppl. Fig. 5B**), further corroborating its senescent phenotype.

Validation of the senescent *p21* cell subpopulation at the protein expression level included the development of a *p21*-tdTomato (*p21*-tdTom) reporter mouse model. *p21*-tdTom mice were generated by CRISPR/Cas9-mediated knock-in of a P2A-tdTomato cassette into the 3'-end of the endogenous *p21* gene in a bicistronic fashion, leading to the production of two different proteins, P21 and tdTomato, from the same transcript (**Fig. 2A**). Metabolic evaluation of p21-tdTom reporter showed no difference between genders and with respect to wild type mice in glucose clearance (**Suppl. Fig. 6 A, B**). Doxorubicin treatment increased *Cdkn1a* expression and decreased *Pdx1* expression in both islets from reporter and non-reporter mice (**Suppl. Fig. 5 C, F**) showing that gene expression was not affected by the transgene construct (**Suppl. Fig 5 H, I**). Insulin content was also not affected by the reporter (**Suppl. Fig. 5 J**). Pancreatic islets isolated from these mice had detectable tdTom-expressing β-cells, as shown by immunohistochemistry (**Fig. 2B**) and live fluorescence microscopy (**Fig. 2C, C'**), confirming effective protein translation. There was a 67% overlap between p21 protein by immunostaining and tdTom red signal by flow cytometry (**Fig. 2D, Suppl. Fig 7**).

To test the age dependency of the p21 subpopulation, islets from young (3 months old) and aged (18 months old) *p21*-tdTomato mice were dispersed into single cells. p16 was detected by immunostaining and p21 was detected by endogenous Tomato fluorescence. All three subpopulations detected in the scRNAseq data were also detected at the protein level in islets from 3-month-old mice (**Suppl. Fig 8**) in the following proportions: 18% $p21^+$ and 4% $p16^+$, supporting the scRNASeq results. The $p21^+$ subpopulation significantly increased with age to 28%.

The function of the $p21^+$ subpopulation was evaluated by isolating and dispersing islets from aged adult male and female *p21*-tdTomato mice (51-72 weeks of age). Flow cytometry was used to separate cells into *p21*-$tdTOM^-$ and *p21*-$tdTOM^+$ subpopulations, and the response to glucose was evaluated with glucose-stimulated insulin secretion (GSIS) (**Fig. 2E**). Senescent *p21*-$tdTOM^+$ cells had impaired glucose responsiveness, as shown by a decreased insulin secretion index (insulin secretion at 16.8 mM glucose/insulin secretion at 2.6 mM glucose) (**Fig. 2F**) due to increased basal insulin secretion (**Fig. 2G**), a feature typical of dysfunctional β-cells (6-8).

To assess whether the decreased expression of genes related to β-cell identity and function observed in the *Cdkn1a*$^+$ subpopulation was reflected at the protein level, pancreatic sections from *p21*-tdTomato mice were stained for the following antigens and their intensity quantified: MAFA, PDX1, and NKX6.1. The results showed a significant decrease in the protein levels of these β-cell transcription factors in islets with high levels of tdTOM compared with islets with low levels of tdTOM, as assessed by semi-quantitative immunofluorescence (**Fig. 2H, J**), confirming loss of cellular identity. Furthermore, HMGB1, another marker of cellular senescence, showed predominant

nuclear exclusion in islets with high tdTOM levels (**Fig. 2I, 2J**) supporting its senescent identity.

In summary, these analyses identified a *Cdkn1a*$^{+}$ (encoding *p21*) β-cell subpopulation that exhibited low glucose responsiveness, loss of β-cell identity, and increased expression of well-known senescence and SASP genes.

Non-cell autonomous effects of the β-cell SASP induce secondary senescence

To assess whether SASP factors from senescent β-cells had non-autonomous effects on non-senescent β-cells and contribute to senescence, a series of experiments were conducted using complete conditioned media (CM) containing either the full SASP from senescent cells, a selection of 4 SASP factors or individual SASP factors.

For complete CM experiments, a mouse insulinoma cell line, (MIN6) was treated with CM from senescent and non-senescent cells. CM from senescent cells was generated by treating MIN6 cells, with the DNA-damaging agent, bleomycin, which induces senescence and SASP secretion *in vitro* (1). Conditioned media from vehicle-treated cells (CCM) or bleomycin treated cells (BCM), were collected and used to treat naïve MIN6 cells for 24 h. Five days after exposure to CCM or BCM, cells were collected and expression of senescence markers and proliferation were analyzed (**Fig. 3A**). Exposure to BCM resulted in increased *p16* expression (**Fig. 3B**) and a marginal increase in β-gal activity (**Fig. 3C**), both of which are senescence markers (9).

Proliferative arrest, an additional indicator of senescence, was analyzed by measuring Ki67 staining intensity in individual nuclei using ImageJ. A frequency distribution graph of Ki67 intensity revealed two main subpopulations: a non-proliferative cells (*Ki67* intensity

206 <10 AU, as measured with image analysis software) and proliferative cells (Ki67
207 intensity>100 AU) (**Fig. 3D, E**). MIN6 cells treated with conditioned media obtained from
208 cells previously treated with bleomycin (BCM), had a greater percentage of
209 nonproliferating cells and a lower percentage of proliferating cells, suggesting induction
210 of senescence. These findings support a non-cell autonomous effect of the SASP,
211 capable of inducing secondary senescence.

212 To analyze non-cell autonomous effects of individual SASP in β-cells, four factors were
213 selected based on the following criteria: 1) previously published as a senolytic target
214 and/or SASP factor; 2) identified as a SASP factor secreted by β-cells in our proteomic
215 analysis (1); 3) common factor between mouse and human SASP and/or reported
216 increase in β-cells from donors with T2D (1); and 4) measured concentration in plasma
217 by immunoassay as reported in the Human Protein Atlas (**Table 1 and Suppl. Table 2**).
218 The following SASP factors met these criteria and were preferentially transcribed by
219 *Cdkn1a*$^{+}$ cells: LSAMP, IDE, DUSP3, GDF15.

220 To test the dependency of these SASP factors on *p21*, a conditional siRNA knockdown
221 was developed. At the protein level, conditional downregulation of *p21* led to significant
222 decreases in IDE and LSAMP (**Fig. 3F**). At the transcriptional level, a significant positive
223 correlation was observed between *Lsamp*, *Dusp3*, *Gdf15*, and *Ide,* and the mRNA levels
224 of *p21* (**Fig. 3G-J**). These patterns show that the chosen SASP factors directly correlated
225 with the CDK inhibitor, *p21*, thereby supporting subpopulation specificity.

226 To test the non-cell autonomous effects of *p21*-SASP factors, islets were isolated from
227 male and female *p21*-tdTOM mice and incubated with a combination of *Cdkn1a*$^{+}$ SASP
228 factors (LSAMP, DUSP3, GDF15, and IDE) for 5 days before assessing senescence and

function (**Fig. 3K**). Protein concentration levels were determined by reported circulating levels in humans in the Human Protein Atlas, however, the paracrine concentrations are likely higher than those reported in plasma but impossible to measure with currently available technology. SASP from *Cdkn1a*$^{+}$ cells significantly increased the p21 subpopulation as measured by flow cytometry (**Fig. 3L, Suppl. Fig. 7**) and upregulated *p21* mRNA (**Fig. 3M**) while downregulating the key β-cell genes: *Mafa, Pdx1*, and *Ins1*. At the functional level, *p21*-SASP factors impaired β-cell function, as reflected by a lack of glucose responsiveness (**Fig. 3N**), characterized by increased basal insulin secretion (**Fig. 3O**).

To test whether individual *p21*-SASP factors were able to induce secondary senescence, MIN6 cells were treated with individual proteins for 4 days. All four proteins upregulated expression of 6 senescence and SASP genes (*p21, p16, Igf1r, Il1a, Il6, and Lsamp*) (**Fig. 3P-S**); LSAMP was the individual factor that induced the greatest increases in expression of senescence genes (**Fig. 3Q**).

These results indicate that SASP factors induced secondary senescence in islet cells in a pathway-specific way: SASP released from p21^{+} cells increased the p21 subpopulation. SASP factors induced senescence both in combination and individually, implying that a small percentage of senescent p21^{+} β-cells can induce secondary senescence and loss of β–cell identity. Based on these findings, the β-cell SASP can be considered an additional therapeutic target for restoring β-cell identity and functionality.

siRNA-mediated *p21* knockdown improves insulin secretion

To evaluate the temporal patterns of *p21* and *p16* expression in β-cells, mouse pancreatic islets were isolated, and a time-course expression was delineated during 12 days in culture (**Fig. 4A**). In control (Scr-siRNA) conditions (**Fig. 4B**), *p21* increased from days 6-10 while *p16* peaked later, at day 10. When *p21*-siRNA was used to keep levels down, the *p16* peak occurred earlier, at day 6 (**Fig. 4B**). This timeframe is consistent with loss of identity and function in $p21^{+}$ β-cells, since the conditional knockdown improved β-cell function (**Fig. 4C**) and increased expression of key β-cell genes at Day 6 (**Fig. 4D**). To examine the role of *p21* and *p16*, in the induction of secondary senescence, these genes were knocked down with siRNA in islet cells exposed to *p21*-SASP factors (LSAMP+DUSP3+GDF15+IDE) (**Fig. 4E, Suppl. Fig. 9A**). From a functional perspective, *p21*-siRNA improved β-cell function under basal conditions but did not rescue the functional loss induced by SASP (**Fig. 4F**) Ins1 nor Mafa transcription (**Fig. 4L, M**), suggesting additional *p21*-indedpendent pathways leading to functional and identity loss in secondary senescence. From a transcriptional perspective, knocking down *p21* significantly decreased *p21*-SASP induced expression (**Fig. 4G**) with no significant changes in *p16* expression (**Fig. 4H**). Instead, *Mdm2* (p53 negative regulator) (**Fig. 4N**) and *Casp3* (apoptosis) (**Fig. 4K**) were upregulated. Proliferation genes *Mki67* and *Pcna* (**Fig. 4O, P**). Overall, these changes suggest that in the absence of *p21*, SASP factors induce alternate cell fates such as apoptosis and/or proliferation. These possibilities should be explored further.

When *p16* was knocked down in islets exposed to *p21*-SASP factors (**Suppl. Fig 9A, B**) there was an increase in *p21* expression (**Supl. Fig 9C**), with no significant changes in other senescence markers: *p53, Bcl2* and *Mdm2* (**Suppl. Fig. 9D, E, F**). These results

suggest that in the absence of *p16*, senescence might be induced through the *p21* pathway.

JAK inhibitors restored β-cell function, transcriptional identity, and cell subpopulations in mouse islets

SASP secretion and action are known to be regulated by several pathways (10), including the Bromodomain and Extra-Terminal domain (BET) pathway, whose regulation was queried in mouse senescent β-cells (6). A significant and prominent upregulation of the JAK/STAT pathway (**Fig. 5A, Suppl. Fig. 10**) was identified compared with non-senescent β-cells, and JAK inhibitors (JAKi) were tested *in vitro* and *in vivo* (**Fig. 5B**) to assess their efficacy in maintaining β-cell function and identity while decreasing SASP and secondary senescence.

In vitro, JAK1/2i attenuated the effects of *p21*-SASP factors by decreasing the p21 and p16 subpopulations of senescent cells measured by flow cytometry (**Fig. 5C, Suppl. Fig. 7**). At the transcriptional level, JAK1/2i decreased all tested senescence and SASP genes in islets treated with *p21*-SASP factors (**Fig. 5D**), while upregulating *Mafa*, a key transcription factor for β-cell function. These positive transcriptional and subpopulation changes were reflected at the functional level. Concurrent treatment of mouse islets with *p21*-SASP factors and JAK1/2i restored the secretion index, indicating improved β-cell functionality (**Fig. 5E**).

The effects of JAK inhibitors were also evaluated *in vivo* with a model of insulin resistance in which mice were fed a high-fat diet (HFD) that increases senescence in β-cells (6) and other metabolically relevant tissues (11). Young (8-week-old) *C57Bl/6N* male mice were

fed a HFD during 6 weeks. They received an osmotic pump containing vehicle or a JAK1/2i for the last 4 weeks (**Fig. 5B**). Downregulation of the JAK pathway was confirmed at a transcriptional level ($p<0.02$), with no differences in the SMAD/Activin pathway, which can be modulated by JAKi. Bulk RNA-Seq of islets isolated from animals in the different treatment groups showed *Cdkn1a* induction by HFD (**Fig. 5F**). Also, HFD increased p21 protein levels, which were suppressed by treatment with JAK1/2i (**Fig. 5G, H**). At the transcriptomic levels, increased expression of senescence and SASP genes (**Fig. 5I**) and decreased expression of β-cell hallmark identity and functional genes (**Fig. 5J**) were observed with HFD, which were restored by JAK1/2i. Functionally, JAK1/2i restored glucose responsiveness lost after HFD *in vivo,* as evaluated during an intraperitoneal glucose tolerance test (IPGTT) (**Fig. 5K**) and increased circulating insulin levels (**Fig. 5L**).

The peripheral effects of JAK1/2i were evaluated using qPCR in the following metabolically relevant tissues: liver, visceral adipose tissue, and skeletal muscle (**Suppl. Fig. 11**). JAK 1/2i did not have a significant effect on the expression of senescence or SASP genes at the doses used (12.5 mg/kg/day), suggesting a preferential effect on β-cells.

These results showed that JAKi decreased senescence genes and subpopulations while restoring β-cell function and transcriptional identity in mouse β-cells, both *in vitro* and *in vivo*.

Human 21$^+$ β-cells are dysfunctional and lose transcriptional identity

Analysis of the relevance of the *p21*$^+$ β-cell population to human islets and disease included data from the Human Islets Database (12). *CDKN1A* transcript levels were

317 significantly increased in islets from donors with type 2 diabetes (T2D) compared to islets
318 from donors without diabetes (**Fig. 6A**). Additionally, there was a negative correlation
319 between P21 protein levels and insulin secretion index (**Fig. 6B**), suggesting that human
320 $p21^+$ β-cells are also dysfunctional.

321 To further profile and map *p21*$^+$ β-cells in human islets, whole pancreas and human islets
322 were obtained as part of the SenNet KAPP-Sen Tissue Mapping Center (**Fig. 6C**).
323 Isolated islets from donors without diabetes across the lifespan underwent scRNASeq for
324 transcriptomic analysis, Xenium for spatial transcriptomic and CODEX for spatial
325 proteomic analysis. The proportion of $p21^+$ β-cells in samples from donors without
326 diabetes was 37% per scRNASeq (10 donors, aged 34-64 years), 15% by Xenium and
327 7% by CODEX (13 donors, aged 21-71 years). These differences might reflect different
328 sensitivity per platform as well as higher senescence induction due to the islet isolation
329 procedure prior to scRNASeq.

330 Key β-cell identity and functional genes (*INS, NKX6.1*) were significantly downregulated
331 in the *CDKN1A*$^+$ β-cell subpopulation when compared to non-senescent and *CDKN2A*$^+$
332 β-cells (**Fig. 6D, E**). To understand whether these senescent subpopulations may have
333 originated from independent lineages or from a single population that expresses these
334 markers in a temporally distinct fashion, as previously suggested by us and others (1, 13,
335 14), pseudotime analysis of scRNASeq was performed in human β-cells. Seven states
336 were identified during the progression of a human non-senescent β-cell to a senescent
337 state (**Fig. 6F, G**), with states 5, 6, and 7 showing upregulation of key senescent genes:
338 *TP53, CDKN1A*, and *CDKN2A* (**Fig. 6G**). State 5 expressed higher levels of *TP53*, state

6 of *CDKN1A* and state 7 of *CDKN2A*, suggesting a temporal progression of β-cells through these three senescent stages. In support of these being senescent states, 5, 6, and 7 had significantly higher senescence scores using the GO term (**Fig. 6H**) and senescence Fridman (**Fig. 6I**) gene data sets.

Given the correlation between p21 with T2D and islet dysfunction in humans, spatial proteomic (CODEX) and transcriptomic (Xenium) analysis focused on CDKN1A/p21^{+} β-cells from fixed whole pancreas. P21 expression was divided into quartiles (Q), with Q1 having the lowest levels and Q4 the highest. At the protein level, β-cells with higher levels of P21 also had higher levels of other senescence markers: HMGB1, and XP53BP1 (**Fig. 6J**). Consistent with their loss of identity, this same population had lower levels of key β-cell proteins: INSULIN and C-PEPTIDE (**Fig. 6M**). At the transcriptomic level, β-cells with the highest levels of nuclear *CDKN1A* had the lowest levels of *INSULIN* and *MAFA*, a key functional transcription factor (**Fig. 63K, L**). These correlations were maintained when β-cells were selected based on nuclear protein P21 levels and their transcriptional mapping revealed lower levels of *INSULIN* and *MAFA* mRNA transcripts (**Fig. 6N**).

These results demonstrate that a senescent and dysfunctional subpopulation of p21^{+} β-cells can be identified in human islets. These cells are more abundant in tissues from individuals with T2D and thus may contribute to β-cell dysfunction and T2D pathogenesis.

Pharmacological JAK inhibition restored function of human β-cells

To analyze the relevance of JAK inhibition in human β-cells as a potential regulator of secondary senescence, data from the Human Islet Program was used (12). JAK1 protein levels were increased in islets from donors with T2D compared to islets from donors without diabetes (**Fig. 7A**). Additionally, there was an inversely negative correlation between JAK1 protein levels and secretion index (**Fig. 7B**), suggesting that human JAK1 might be a potential target to restore β-cell function in islets with higher levels of $P21^{+}$.

Several JAK inhibitors are approved for clinical use for different diseases (*e.g.*, rheumatoid arthritis). Deidentified A1c levels were obtained from the Joslin Adult Clinic from a limited number of adults with T2D who were also prescribed a JAKi (**Fig. 7C**). Analysis of the longitudinal A1c of each patient, revealed that individuals taking JAK1i and JAK1/2i had a 1% decrease in A1c levels compared to levels before the drug was prescribed (**Fig. 7D**).

Based on this rationale, the role JAK1/2i was tested in human islets.

Islets from human donors (**Suppl. Table 3**) were treated *in vitro* with JAK1/2i for 4 days, after which CM was collected for aptamer-based proteomic analysis of the SASP (**Fig. 7E**). The top upregulated (**Fig. 7F**) human SASP proteins identified in human β-cells (1) were compared between CM from control human cells to CM from human cells treated with JAK1/2i. Treatment with JAK1/2i resulted in a significant decrease in the secretion of SASP proteins (**Fig. 7F, G**)**,** demonstrating its effectiveness in targeting human SASP.

To analyze the effects of SASP inhibition on senescent subpopulations, islets from donors without diabetes (were $P21^{+}$ cells and a functional SASP are also found (1)) were treated as described above and analyzed for the expression of *P21* mRNA, which was decreased

by JAK1/2i (**Fig. 7H**). This was accompanied by an increase in the secretion index in islets from donors without T2D (**Fig. 7I**). Due to limited islet supply and the presence of senescent β-cells in islets from donors of all ages, we have included a range of ages and metabolic conditions to support the pathophysiological importance of this population.

To test whether the JAK pathway was also relevant in a diseased state, islets from donors with T2D were treated with JAK1/2i for four days. *P21* transcription was significantly decreased (**Fig. 7J**). From a functional perspective, JAK1/2i restored insulin secretion dynamics in the islets from two donors with T2D (58, 55 years old with BMI 38, 42 respectively) (**Fig. 7K,L**). This can be seen as a restoration of first-phase insulin secretion and an enhanced response to the secretagogue, IBMX. Furthermore, improvement in insulin secretion was observed not only in perifusion but also in static GSIS, and similar effects were observed with two JAK1/2i drugs (**Fig. 7M**).

In conclusion, the human β-cell SASP is a therapeutic target to restore function during progression and in established T2D.

DISCUSSION

The importance of heterogeneity in cellular senescence is increasingly being recognized as a key factor in developing better-targeted interventions for various diseases. *p21* (encoded by *Cdkn1a*) and *p16* (encoded by *Cdkn2a*) are well-established markers and effectors of senescence, and their expression patterns have been used to define three different subpopulations of β-cells. We found that $p21^{+}$ cells are the predominant senescent subpopulation of β-cells in models of metabolic stress, T2D, and aging.

Interestingly, the gene expression profile of these cells differed from that of p16^{+} cells: *Cdkn1a*$^{+}$ β-cells were characterized by reduced expression of hallmark genes associated with β-cell identity and function, along with increased expression of commonly described SASP genes (6).

The co-expression of other markers of senescence and increased transcription of SASP factors support this is a *bona fide* senescent population rather than a population undergoing transient stress. The expression dynamics observed in islets from mice treated with S961 for two weeks suggested that *Cdkn1a* could be an initial driver of β-cell senescence, while *Cdkn2a* would increase at a later stage, a process that has also been previously proposed by us and others (1, 14). This concept was further supported by pseudotime analysis of mouse and human scRNASeq of β-cells, by *Cdkn2a*$^{+}$ cells distinctly separating from *Cdkn1a*$^{+}$ and the non-senescent cells in the PCA plot, and by the conditional knockdown *of p21* in mouse islets. Even though these populations are temporally asynchronous, their specific control should be studied further.

Our data support the induction of secondary senescence in β-cells by *Cdkn1a*$^{+}$ cells. This effect was shown with full SASP in conditioned media, with a subset of selected SASP factors and by each factor individually. In these different conditions, naïve cells exposed to SASP exhibited increased expression of senescence genes (particularly *p21*) and became dysfunctional, consistent with secondary senescence being an important effector of β-cell dysfunction in models of insulin resistance and progression to T2D. The role of the β-cell SASP as an inducer of secondary senescence underscores the importance of therapeutically targeting the secretome of senescent cells through pharmacological interventions. Treatment of β-cells with the JAK1/2i decreased the expression of

senescence markers and improved cell function in models of early T2D. JAK1/2i, compete with Janus tyrosine kinases 1 and 2 to reduce the intracellular signalling of cytokines and growth factors, thereby mitigating their transcriptional effects (15, 16). In human β-cells, JAKi significantly decreased secretion of SASP factors and, based on RNASeq data, it also significantly decreased signalling by interleukins (IL2, 6, 9, 20, 21 27, 28, 35), IFNγ, and TP53 activity in mice. Similar inhibition by JAKi has been reported in the adipose tissue (17). The specific roles of each of these pathways in restoring the function and identity of β-cells will be subject of future studies.

If JAK inhibitors are considered as an additional strategy to restore β-cell function during progression to T2D, several points deserve reflection given their multiple downstream effects. The JAK/STAT pathway plays a dual role in β-cells, underscoring the need for selective modulation. Prolactin-induced JAK2/STAT5 activation promotes β-cell survival by increasing the expression of anti-apoptotic protein BCL-XL and protects against glucolipotoxicity-induced cell death in rodent and human β-cells (22, 23). This suggests that enhancing JAK2/STAT5 signaling may maintain β-cell mass, but therapeutic strategies must avoid excessive activation that could promote inflammation.

Additionally, the JAK/STAT pathway mediates pro-inflammatory effects in response to extracellular cytokines and chemokines. The IL-6/JAK2/STAT3 pathway has been shown to promote inflammation and endoplasmic reticulum stress in diabetic β-cells (24). Conceptually, it can't be ruled out that JAKi in our models, modulate inflammation given its known effects on the immune system. Consistent with the effects of JAK signaling on the immune system, the main reported side effects of JAKi are infections, particularly viral infections, which can be mitigated with vaccination (25). Increased risk of cardiovascular

449 and thromboembolic events are reported side effects- these could be avoided by
450 specifically targeting these drugs to β-cells through chemical manipulation. Also, some of
451 these effects might be dose dependent.

452 Supporting the use of JAK inhibitors to protect human β-cells, daily administration of
453 JAK1/2i in low doses to people, including children, with recent onset Type 1 diabetes,
454 preserved β-cell function (26), and was well tolerated.

455 In conclusion, senescent β-cell heterogeneity provides the biological basis for
456 differentially targeting specific subpopulations and counteracting their effects on
457 neighbouring cells during diabetes progression. Considering that multiple
458 pharmacological targeting strategies are available, SASP inhibition with JAK inhibitors
459 was shown to restore human β-cell function and enhance cell survival in models of early
460 β-cell dysfunction. These concepts will further our understanding of senescence biology
461 and support the rational development of novel therapeutic strategies for diabetes.

MATERIALS AND METHODS

Sex as a biological variable

Our study examined male and female animals and human samples. Similar findings are reported for both sexes.

Animals

Male *C57BL/6J* mice (8-week-old or 6-9-month-old-retired breeders) obtained from Jackson Labs were used for islet isolation and conditioned media generation. Male mice were chosen at this stage because they are more susceptible to develop insulin resistance after dietary or pharmacological interventions. All experiments were performed in the animal facilities at the Joslin Diabetes Center with approval from its Animal Care and Use Committee. Mice were kept on a 12-hr light/dark cycle with water and food provided *ad libitum*. A housing temperature of 22.2-22.7°C was maintained.

p21-tdTomato Mice

To generate a mouse in which dTomato expression was driven by the *p21* gene, the P2A-dTomato transgene was inserted in place of the stop codon at the 3' end of the coding region. The Easi-CRISPR design methodology was followed as previously published (27, 28). Bioinformatic analysis of the gene for gRNA identification was performed by crispor.tefor.net. Microinjection was performed into embryos from 4-week-old *C57 Bl6* female donors (Jackson), which were subsequently implanted into 6-week-old *Swiss Webster* females (Charles River). Junction sequencing was performed to verify the construct.

IPGTT showed no significant differences among p21-tomato reporter vs non-reporter mice with both sexes in glucose levels (**Suppl. Fig. 5A, B**).

Cell Lines

Murine MIN6 cells were originally provided by Dr. Jun-ichi Miyazaki from Osaka University Medical School, and the sex of the cell line was not available. The cell line was maintained in Dulbecco's modified Eagle's medium (HG, w/4500 mg/L glucose, L-glutamine, sodium pyruvate, and sodium bicarbonate) from Sigma–Aldrich® supplemented with 15% fetal bovine serum (FBS) from Summerlin Scientific©, 1% penicillin–streptomycin (5,000 U/mL) from Gibco™, and 0.05% β-mercaptoethanol (99% cell culture tested) from Sigma–Aldrich®. The cells were incubated at 37°C with 5% CO_2.

Mouse Primary Islets

p21-tdTomato and *C57BL/6N* mice were used for islet isolation. Isolation was performed according to the protocol described by Gotoh, M.*, et al.* (29). The islets were then hand-picked under a StereoZoom® 7 microscope and plated in Petri dishes with islet media. The media were composed of RPMI 1640 (1x, [+] L-glutamine) (Gibco™) supplemented with 10% fetal bovine serum (FBS; Summerlin Scientific) and 1% penicillin–streptomycin (5,000 U/mL; Gibco). For the dispersion of islets, we used TrypLE™ Express Enzyme (1x, [-] Phenol red) (Gibco). The islets were incubated at 37°C with 5% CO_2.

Human Primary Islets

Human islets were obtained from donors through IIDP and Prodo Labs (**Suppl. Table 3**). Immediately upon arrival, the islets were cultured in CMRL Medium 1066 (1x, [-] glutamine) from Gibco™ containing 10% FBS (Summerlin Scientific) and 1% penicillin–

streptomycin (5,000 U/mL) (Gibco). For the dispersion of islets, we used TrypLE™ Express Enzyme (1x, [-] Phenol red) (Gibco). The islets were incubated at 37°C with 5% CO_2.

Whole Pancreas Preparation

Whole pancreata were obtained from the University of Texas Health San Antonio from IRB-exempt brain-dead organ donors and shipped to Joslin Diabetes Center under approved protocols. Donors were screened by the Texas Organ Sharing Alliance (TOSA) according to established criteria, including age 20–60+ years, and excluded for conditions such as type 2 diabetes, pancreatic malignancy, pancreatitis, use of agents with senolytic activity, or infection. Pancreata were sectioned into head, body, tail, and regions along the pancreatic margin, with samples processed as both formalin-fixed paraffin-embedded and frozen tissues for downstream histological and molecular analyses. Tissue preservation and shipping procedures were standardized to ensure sample integrity prior to analysis at Joslin Diabetes Center.

JAK Inhibitor Treatment *in vitro*

The following drug concentrations were used for treatment and were diluted in CMRL Medium 1066 1X (See Human Primary Islets): 1 μM JAK1/2i (momelotinib) and 100 nM JAK1/2i (baricitinib). The concentration of momelotinib was based on published data (17), which showed effective decreases in the transcription of specific SASP factors. Human and mouse cells were incubated for 4 days in wells previously treated with PEI and Geltrex.

JAK Inhibitor Treatment *in vivo*

After two weeks of HFD feeding (60% v/v), the animals (8-week-old male *C57BL/6N* mice) were subdivided into three groups: saline, JAK1/2i momelotinib, vehicle (HFD, 0.9% NaCl), or JAK1/2i (HFD+momelotinib, 12.5 mg/kg/day) administered through an osmotic pump in 8-week old animals. All control animals received vehicle via oral administration (NaCl 0.9%). Blood glucose levels in the mice in all groups were monitored biweekly, and the mice were sacrificed after treatment (4 weeks for HFD). The pancreatic islets were then isolated for qPCR analysis or bulk RNA-seq. Heart blood was collected through cardiac puncture to measure circulating insulin in the mice.

Intraperitoneal Glucose Tolerance Test (IPGTT)

Intraperitoneal glucose tolerance tests (IPGTTs) were performed before and after senolytic or senomorphic treatment, as well as in p21-tdTomato–positive and –negative littermate mice. Following a 6-hour fast, mice received intraperitoneal glucose (2 g/kg body weight), and blood glucose levels were measured at baseline and multiple time points up to 120 minutes post-injection using a glucometer. Blood samples collected at 0 and 15 minutes were additionally used for serum insulin quantification by ELISA.

Generation of SASP-Conditioned Media

MIN6 cells were cultured in T175 flasks and treated with either 50 μM bleomycin or DMSO control for 48 hours to induce senescence. Following treatment, cells were recovered in normal medium for 72–96 hours and subsequently incubated in serum-free medium for 24 hours to generate conditioned media. The collected media were used in downstream experiments as bleomycin-conditioned media (BCM) or control-conditioned media (CCM).

Conditional Knockdown with siRNA

MIN6 cells were transfected with Opti-MEM–based siRNA (50 nM) mixtures using Lipofectamine RNAiMAX and incubated for 48 hours before downstream analyses. For primary mouse islet experiments, dispersed islet cells were cultured overnight and transfected with scrambled or p21-targeting siRNA using similar conditions. Following transfection, media were replaced and cells maintained for 4, 6, 8, 10, and 12 days post-transfection. Functional assessment included glucose-stimulated insulin secretion (GSIS) assays, and RNA was isolated from harvested cells for reverse transcription and quantitative PCR analysis of gene expression.

In vitro Recombinant Protein Treatment

Approximately 300,000 MIN-6 cells were plated into 24-well plates with 500 µL of Dulbecco's modified Eagle's medium supplemented with 15% FBS. The cells were incubated at 37°C with 5% CO_2 for 24 hrs to allow attachment. The concentrations of the following recombinant proteins were compared to those detected in plasma by immunoassay (https://www.proteinatlas.org): DUSP3 (1.3 µg/L), GDF15 (1.3 µg/L), IDE (0.31 µg/L), LSAMP (150 µg/L), HSP90 (71 µg/L), and GSTP1 (69 µg/L). The recombinant proteins were diluted RPMI 1640 media without FBS supplemented with 1% bovine serum albumin (BSA). Details are provided in **Supplementary Table 2**. The cells were treated for 48 hrs, followed by incubation for 48 hrs in normal media. After treatment, the cells were subjected to qPCR.

Glucose-Stimulated Insulin Secretion (GSIS) *in vitro*

Static glucose-stimulated insulin secretion assays were performed using Krebs-Ringer HEPES buffer containing defined concentrations of salts, glucose, and BSA. Islets and/or FACS-sorted cells from P21-tdTom mice were preincubated in low-glucose conditions, followed by sequential low- and high-glucose incubations. Supernatants and corresponding cells were collected after each step for normalization to RNA or DNA content and stored for downstream analyses. Insulin secretion was quantified using ELISA or ultrasensitive HTRF insulin assays.. The raw insulin secretion values at low and high glucose are summarized in **Suppl. Table 7**.

Quantitative Real-Time PCR

RNA extraction was performed using the RNeasy Micro Kit, followed by reverse transcription of RNA to cDNA using SuperScript IV Reverse Transcriptase. Gene expression was quantified by qPCR using PowerUp SYBR Green Master Mix, with β-actin used for normalization. Primer sequences used in the study are provided in the **Suppl. Table 4**.

Immunostaining, Image Acquisition, and Morphometric Analysis

The cells were fixed with 10% formalin and permeabilized with 0.3% Triton X-100 (Alfa Aesar). The cells were blocked with normal donkey serum at a 1:50 dilution in PBS. The sections were incubated overnight at 4°C with anti-Ki67 antibody. The next day, they were incubated with anti-insulin and then with fluorochrome-conjugated secondary antibodies and mounted with Fluoroshield™ with DAPI (Sigma Aldrich).

590 The antibodies used are listed in **Suppl. Table 5**. For each stain, all images were taken
591 with the same settings in confocal mode using a Zeiss LSM 710 microscope such that
592 comparisons across conditions could be made.

593 The intensity for proliferation analysis and the area for cell density were quantified using
594 ImageJ.

595 Quantification of fluorescence intensity was performed through FIJI. TdTOMATO
596 fluorescence was quantified, followed by classification into higher or lower signalling
597 categories based on the mean integrated density. Lower signalling corresponded to
598 values in the lower half of the distribution, whereas higher signalling represented values
599 in the upper half. To address islet heterogeneity, immunostaining was adjusted using the
600 corresponding tdTomato integrated density values. This method facilitated the
601 comparison of the impact of increasing tdTOMATO intensity and, consequently, P21
602 expression and other marker β-cell markers: INSULIN, MAFA, NKX6, and PDX1. Staining
603 details are provided in the **Supplementary data**.

604 **Bulk RNA-Seq**

605 Islet isolation was performed according to the protocol described by Gotoh, M., *et al*. RNA
606 was extracted from isolated islets using a RNeasy Micro Kit and sent for sequencing to
607 DNA Link (Los Angeles, CA). Data analysis was performed by the Bioinformatics and
608 Biostatistics Core at Joslin Diabetes Center.

609 **Single-Cell RNA Sequencing (scRNASeq): Mouse Islets**

610 Our previously published (1) scRNASeq database (GSE149984) was reanalyzed with β-
611 cells clustered into subpopulations using the expression of *Cdkn1a* and *Cdkn2a*. Briefly,

ALZET mini-pumps with the insulin receptor antagonist S961 or PBS were surgically inserted into mice for 2 weeks as described by Aguayo-Mazzucato *et al*.[4]. Three groups of mice (n=4 animals per group) were used: control (PBS pumps), S961 (20 nmol/L/week for 2 weeks), and recovered (mice with S961 removed for 2 weeks) groups. For single-cell RNA sequencing (scRNAseq), islets were isolated from all mice in each group on the same day, cultured overnight, and dispersed. There were 2939 β-cells in the control group, 2896 cells in the S961 group, and 2513 cells in the recovery group.

For βSenMayo, the list of genes described in (5) was assessed in different senescent subpopulations of β-cells from the control condition. Only those genes with quantifiable gene reads in all 3 subpopulations were included in the analysis to exclude those with extremely low expression in β−cells.

A detailed description of the bioinformatic analysis of the scRNAseq data can be found in the **Supplementary Methods**. The accession number for the scRNAseq data is GSE149984.

scRNASeq, CODEX and Xenium of Human Islets

A full description is provided in **Supplementary Data.**

β-Gal Activity Assay

To measure senescence-associated β-galactosidase (SA-βGal) activity, we used the *Dojindo Cell Count Normalization Kit (C544)* combined with the *Cellular Senescence Plate Assay Kit – Spider-βGal (SG05)* following the manufacturer's protocol for combined analysis.

Flow Cytometry

1. β-Gal$^-$ and β-Gal$^+$ Human and Mouse Cells. Human and mouse β-cells were sorted using flow cytometry based on β-Gal activity to divide them into senescent (β-Gal$^+$) and nonsenescent (β-Gal$^-$) populations. B-Gal activity was measured using an Enzo cellular senescence live-cell senescence assay kit (ENZ-KIT130-0010) following the manufacturer's instructions while optimizing the substrate incubation time to 1 hr. Sorting was performed using a DakoCytomation MoFlo Cytometer or FACSAria in the Joslin DRC Flow Cytometry Core. Primary islets were incubated with antibodies against CD45 and CD11b to eliminate immune cells.

2. p21-tdTom mice. Islets from *p21*-tdTomato mice were isolated, dispersed into single cells, and sorted using a MoFlo Cytometer based on Tomato Red fluorescence. The cells were collected in media, plated in 96-well plates overnight, and assessed for glucose-stimulated insulin secretion the following day. The results were normalized to the DNA quantity. A detailed protocol for staining for *p16^{Ink4+}* in FACS is provided in the **Supplementary Methods** and **Suppl. Table 6**. The gating criteria are shown in **Suppl. Fig. 7**, and 90% enrichment of β-cells was achieved, as previously published (6).

Proteomics of Human Conditioned Media From β-Gal$^-$/β-Gal$^+$ Human Cells and Control and JAK1/2i-Treated Islet Cells

After sorting, β-Gal$^+$ and β-Gal$^-$ cells were plated, and conditioned media were generated to compare the SASP secreted by either cell type. Conditioned media from control and pharmacologically treated cells were generated as described above. The generated conditioned media were analysed using SomaScan proteomics at the BIDMC Genomics

Proteomics Core. Proteomic data were normalized, log2-transformed, and analyzed by principal component analysis (PCA) to assess differences among samples. Differentially secreted proteins were identified using Limma, and statistical significance was determined using moderated paired t tests.

Quantification and Statistical Analysis

The data are shown as the mean ± SEM, and p values < 0.05 were considered significant. For statistical analysis, unpaired or paired two-tailed Student's t tests and 2-way ANOVA were used to compare groups. Normality and log normality analyses were performed, and nonparametric statistics (Kruskal–Wallis test, Mann–Whitney test, and Wilcoxon test) were performed when samples did not meet the criteria for a normal distribution. Prism software was used for graphs and statistical analysis (significance and distribution). Data outliers were determined using the Grubbs outlier test or a deviation of more than 2 SDs from the mean.

Study approval

All experiments were conducted at Joslin Diabetes Center with approval of its Animal Care and Use Committee under protocol number 063-2024. Studies involving human pancreas were determined "Not Human Research" (STUDY 00000152) by Joslin's Committee on Human Studies based on lack of access to any identifying information and specimen collection at other institutions.

Data Accessibility

Human proteomic βGal data are available in the GSE150285 dataset, and human data for the control, JAK1/2i datasets are available in the GSE162521 dataset. Also, mouse

S961 treated scRNAseq data are available in the GSE149984, bulk RNASeq HFD +/- JAKi data are available in the GSE294866. Human scRNAseq, CODEX (phenocycler), Xenium and H&E raw datasets are made available for the public via the SenNet Consortium portal (https://data.sennetconsortium.org/). Code associated with processing and analysis will be made available via the SenNet GitHub page (https://github.com/sennetconsortium).

Supporting data values associated with the main manuscript and supplement material, including values for all data points shown in graphs and values behind any reported means are provided as “Supporting Data Values” excel files.

Acknowledgements

The authors thank Jonathan Dreyfuss from Joslin’s Bioinformatic Core for assisting with the data analysis; Angela Wood and Alison Marotta from the Flow Cytometry Core and Erin Keating of Animal Facilities; Stephan Kissler and Taylor Roberts from the JDC Mouse Genomic Core; and Susan Bonner-Weir for insightful discussion, critical reading of the manuscript and support in obtaining human islets from the IIDP.

This work includes data and/or analyses from **HumanIslets.com** funded by the Canadian Institutes of Health Research, JDRF Canada, and Diabetes Canada (5-SRA-2021-1149-S-B/TG 179092) with data from islets isolated by the Alberta Diabetes Institute Islet Core with the support of the Human Organ Procurement and Exchange program, Trillium Gift of Life Network, BC Transplant, Quebec Transplant, and other Canadian organ procurement organizations with written informed donor consent as approved by the Human Research Ethics Board at the University of Alberta (Pro00013094).

Human islets were provided by the NIDDK-funded Integrated Islet Distribution Program (IIDP) at the City of Hope and from Prodo Laboratories, Inc., in Aliso Viejo, CA.

Funding

This work is the result of NIH funding, in whole or in part, and is subject to the NIH Public Access Policy. Through acceptance of this federal funding, the NIH has been given a right to make the work publicly available in PubMed Central.

- NIH 1R01DK132535, Thomas J Beatson Jr Foundation grant 2020-010, Richard and Susan Smith Family Foundation Award, Institutuional Startup Funds to CAM.
- NIH/NIA U54AG075941 SenNet Initiative, KAPPSen Tissue Mapping Center. MPI GK, NM, PR, VG
- NIH (P30DK036836 to the Joslin Diabetes Research Center).
- NIH 1R25DK113652 to SP
- NIH R25 DK140752 to SL
- NIH R37 AG13925, Hevolution grant HF-GRO-23-1199148-3, and the Connor Fund, Robert and Theresa Ryan, and the Noaber Foundation to JLK and TT grant,
- The Mampei Suzuki Diabetes Foundation and a Mary K. Iacocca Fellowship to KI.
- NIH 2UC4DK098085 to IIDP

Author contributions

CA, PC, KI, FH, SP, SS, SL and MJ acquired, analyzed, and interpreted the data and wrote, edited, and revised the manuscript. AM generated the *p21*-tdTomato mice with the

assistance of the mouse genomic core at Joslin, and HP analyzed the proteomic, scRNAseq, and RNA-seq data. CAM designed the project; acquired, analyzed, and interpreted the data; and wrote, edited, and revised the manuscript.

SenNet KAPPSen members: JAD, DB, SD, SE, AP, FGC, JC, GAK, NM, PR, TT, JLK, VG, JLW contributed to organ retrieval, scRNASeq, CODEX, and Xenium on whole human pancreas and human islets.

All authors read, revised and approved the manuscript.

Competing interests

Part of the work in this manuscript has been submitted for a patent JDP-216 on January 16, 2024, as a US Provisional, 63,621,239.

References

1. Midha A, Pan H, Abarca C, Andle J, Carapeto P, Bonner-Weir S, et al. Unique human and mouse beta-cell senescence-associated secretory phenotype (SASP) reveal conserved signaling pathways and heterogeneous factors. *Diabetes.* 2021.
2. Shrestha S, Erikson G, Lyon J, Spigelman AF, Bautista A, Manning Fox JE, et al. Aging compromises human islet beta cell function and identity by decreasing transcription factor activity and inducing ER stress. *Sci Adv.* 2022;8(40):eabo3932.
3. Helman A, Klochendler A, Azazmeh N, Gabai Y, Horwitz E, Anzi S, et al. p16(Ink4a)-induced senescence of pancreatic beta cells enhances insulin secretion. *Nat Med.* 2016;22(4):412-20.
4. Wang B, Wang L, Gasek NS, Zhou Y, Kim T, Guo C, et al. An inducible p21-Cre mouse model to monitor and manipulate p21-highly-expressing senescent cells in vivo. *Nat Aging.* 2021;1(10):962-73.
5. Saul D, Kosinsky RL, Atkinson EJ, Doolittle ML, Zhang X, LeBrasseur NK, et al. A new gene set identifies senescent cells and predicts senescence-associated pathways across tissues. *Nat Commun.* 2022;13(1):4827.
6. Aguayo-Mazzucato C, Andle J, Lee TB, Jr., Midha A, Talemal L, Chipashvili V, et al. Acceleration of beta Cell Aging Determines Diabetes and Senolysis Improves Disease Outcomes. *Cell Metab.* 2019;30(1):129-42 e4.
7. Aguayo-Mazzucato C, van Haaren M, Mruk M, Lee TB, Jr., Crawford C, Hollister-Lock J, et al. beta Cell Aging Markers Have Heterogeneous Distribution and Are Induced by Insulin Resistance. *Cell Metab.* 2017;25(4):898-910 e5.
8. Aguayo-Mazzucato C, Zavacki AM, Marinelarena A, Hollister-Lock J, El Khattabi I, Marsili A, et al. Thyroid hormone promotes postnatal rat pancreatic beta-cell development and glucose-responsive insulin secretion through MAFA. *Diabetes.* 2013;62(5):1569-80.
9. Dimri GP, Lee X, Basile G, Acosta M, Scott G, Roskelley C, et al. A biomarker that identifies senescent human cells in culture and in aging skin in vivo. *Proc Natl Acad Sci U S A.* 1995;92(20):9363-7.
10. Zhang L, Pitcher LE, Prahalad V, Niedernhofer LJ, and Robbins PD. Targeting cellular senescence with senotherapeutics: senolytics and senomorphics. *FEBS J.* 2023;290(5):1362-83.
11. Wang L, Wang B, Gasek NS, Zhou Y, Cohn RL, Martin DE, et al. Targeting p21(Cip1) highly expressing cells in adipose tissue alleviates insulin resistance in obesity. *Cell Metab.* 2022;34(1):186.
12. Ewald JD, Lu Y, Ellis CE, Worton J, Kolic J, Sasaki S, et al. HumanIslets.com: Improving accessibility, integration, and usability of human research islet data. *Cell Metab.* 2025;37(1):7-11.
13. Sturmlechner I, Zhang C, Sine CC, van Deursen EJ, Jeganathan KB, Hamada N, et al. p21 produces a bioactive secretome that places stressed cells under immunosurveillance. *Science.* 2021;374(6567):eabb3420.
14. De Cecco M, Ito T, Petrashen AP, Elias AE, Skvir NJ, Criscione SW, et al. L1 drives IFN in senescent cells and promotes age-associated inflammation. *Nature.* 2019;566(7742):73-8.
15. Bousoik E, and Montazeri Aliabadi H. "Do We Know Jack" About JAK? A Closer Look at JAK/STAT Signaling Pathway. *Front Oncol.* 2018;8:287.
16. Qureshy Z, Johnson DE, and Grandis JR. Targeting the JAK/STAT pathway in solid tumors. *J Cancer Metastasis Treat.* 2020;6.
17. Xu M, Tchkonia T, Ding H, Ogrodnik M, Lubbers ER, Pirtskhalava T, et al. JAK inhibition alleviates the cellular senescence-associated secretory phenotype and frailty in old age. *Proc Natl Acad Sci U S A.* 2015;112(46):E6301-10.

18. Chan E, Luwor R, Burns C, Kannourakis G, Findlay JK, and Ahmed N. Momelotinib decreased cancer stem cell associated tumor burden and prolonged disease-free remission period in a mouse model of human ovarian cancer. *Oncotarget.* 2018;9(24):16599-618.
19. Abubaker K, Luwor RB, Zhu H, McNally O, Quinn MA, Burns CJ, et al. Inhibition of the JAK2/STAT3 pathway in ovarian cancer results in the loss of cancer stem cell-like characteristics and a reduced tumor burden. *BMC Cancer.* 2014;14:317.
20. Giordano G, Parcesepe P, D'Andrea MR, Coppola L, Di Raimo T, Remo A, et al. JAK/Stat5-mediated subtype-specific lymphocyte antigen 6 complex, locus G6D (LY6G6D) expression drives mismatch repair proficient colorectal cancer. *J Exp Clin Cancer Res.* 2019;38(1):28.
21. Liu T, Li A, Xu Y, and Xin Y. Momelotinib sensitizes glioblastoma cells to temozolomide by enhancement of autophagy via JAK2/STAT3 inhibition. *Oncol Rep.* 2019;41(3):1883-92.
22. Kondegowda NG, Mozar A, Chin C, Otero A, Garcia-Ocana A, and Vasavada RC. Lactogens protect rodent and human beta cells against glucolipotoxicity-induced cell death through Janus kinase-2 (JAK2)/signal transducer and activator of transcription-5 (STAT5) signalling. *Diabetologia.* 2012;55(6):1721-32.
23. Fujinaka Y, Takane K, Yamashita H, and Vasavada RC. Lactogens promote beta cell survival through JAK2/STAT5 activation and Bcl-XL upregulation. *J Biol Chem.* 2007;282(42):30707-17.
24. Li Y, Wang D, Liu Y, Liu C, Chen M, Li J, et al. Tanshinone IIA ameliorates pancreatic injury in type 2 diabetic mice by modulating inflammation and endoplasmic reticulum stress via the IL-6/JAK2/STAT3 pathway. *Funct Integr Genomics.* 2025;25(1):205.
25. Tefferi A, Pardanani A, and Gangat N. Momelotinib (JAK1/JAK2/ACVR1 inhibitor): mechanism of action, clinical trial reports, and therapeutic prospects beyond myelofibrosis. *Haematologica.* 2023;108(11):2919-32.
26. Waibel M, Wentworth JM, So M, Couper JJ, Cameron FJ, MacIsaac RJ, et al. Baricitinib and beta-Cell Function in Patients with New-Onset Type 1 Diabetes. *N Engl J Med.* 2023;389(23):2140-50.
27. Miura H, Quadros RM, Gurumurthy CB, and Ohtsuka M. Easi-CRISPR for creating knock-in and conditional knockout mouse models using long ssDNA donors. *Nat Protoc.* 2018;13(1):195-215.
28. Quadros RM, Miura H, Harms DW, Akatsuka H, Sato T, Aida T, et al. Easi-CRISPR: a robust method for one-step generation of mice carrying conditional and insertion alleles using long ssDNA donors and CRISPR ribonucleoproteins. *Genome Biol.* 2017;18(1):92.
29. Gotoh M, Maki T, Satomi S, Porter J, Bonner-Weir S, O'Hara CJ, et al. Reproducible high yield of rat islets by stationary in vitro digestion following pancreatic ductal or portal venous collagenase injection. *Transplantation.* 1987;43(5):725-30.
30. Scrucca L, Fop M, Murphy TB, and Raftery AE. mclust 5: Clustering, Classification and Density Estimation Using Gaussian Finite Mixture Models. *R J.* 2016;8(1):289-317.
31. Ritchie ME, Phipson B, Wu D, Hu Y, Law CW, Shi W, et al. limma powers differential expression analyses for RNA-sequencing and microarray studies. *Nucleic Acids Res.* 2015;43(7):e47.
32. Johnson WE, Li C, and Rabinovic A. Adjusting batch effects in microarray expression data using empirical Bayes methods. *Biostatistics.* 2007;8(1):118-27.
33. Curran AM, Scott-Boyer MP, Kaput J, Ryan MF, Drummond E, Gibney ER, et al. A proteomic signature that reflects pancreatic beta-cell function. *PLoS One.* 2018;13(8):e0202727.
34. Farris W, Mansourian S, Chang Y, Lindsley L, Eckman EA, Frosch MP, et al. Insulin-degrading enzyme regulates the levels of insulin, amyloid beta-protein, and the beta-amyloid precursor protein intracellular domain in vivo. *Proc Natl Acad Sci U S A.* 2003;100(7):4162-7.
35. Fernandez-Diaz CM, Merino B, Lopez-Acosta JF, Cidad P, de la Fuente MA, Lobaton CD, et al. Pancreatic beta-cell-specific deletion of insulin-degrading enzyme leads to dysregulated insulin secretion and beta-cell functional immaturity. *Am J Physiol Endocrinol Metab.* 2019;317(5):E805-E19.

828 36. Panico K, and Forti FL. Proteomic, cellular, and network analyses reveal new DUSP3 interactions
829 with nucleolar proteins in HeLa cells. *J Proteome Res.* 2013;12(12):5851-66.
830 37. Russo LC, Farias JO, and Forti FL. DUSP3 maintains genomic stability and cell proliferation by
831 modulating NER pathway and cell cycle regulatory proteins. *Cell Cycle.* 2020;19(12):1545-61.
832 38. Vandereyken M, Jacques S, Van Overmeire E, Amand M, Rocks N, Delierneux C, et al. Dusp3
833 deletion in mice promotes experimental lung tumour metastasis in a macrophage dependent
834 manner. *PLoS One.* 2017;12(10):e0185786.
835 39. Basisty N, Kale A, Jeon OH, Kuehnemann C, Payne T, Rao C, et al. A proteomic atlas of
836 senescence-associated secretomes for aging biomarker development. *PLoS Biol.*
837 2020;18(1):e3000599.
838 40. Tanaka T, Biancotto A, Moaddel R, Moore AZ, Gonzalez-Freire M, Aon MA, et al. Plasma
839 proteomic signature of age in healthy humans. *Aging Cell.* 2018;17(5):e12799.
840 41. Fujita Y, Taniguchi Y, Shinkai S, Tanaka M, and Ito M. Secreted growth differentiation factor 15
841 as a potential biomarker for mitochondrial dysfunctions in aging and age-related disorders.
842 *Geriatr Gerontol Int.* 2016;16 Suppl 1:17-29.
843 42. Guo Y, Ayers JL, Carter KT, Wang T, Maden SK, Edmond D, et al. Senescence-associated tissue
844 microenvironment promotes colon cancer formation through the secretory factor GDF15. *Aging*
845 *Cell.* 2019;18(6):e13013.
846 43. Ost M, Igual Gil C, Coleman V, Keipert S, Efstathiou S, Vidic V, et al. Muscle-derived GDF15 drives
847 diurnal anorexia and systemic metabolic remodeling during mitochondrial stress. *EMBO Rep.*
848 2020;21(3):e48804.
849 44. Chung HK, Ryu D, Kim KS, Chang JY, Kim YK, Yi HS, et al. Growth differentiation factor 15 is a
850 myomitokine governing systemic energy homeostasis. *J Cell Biol.* 2017;216(1):149-65.

851

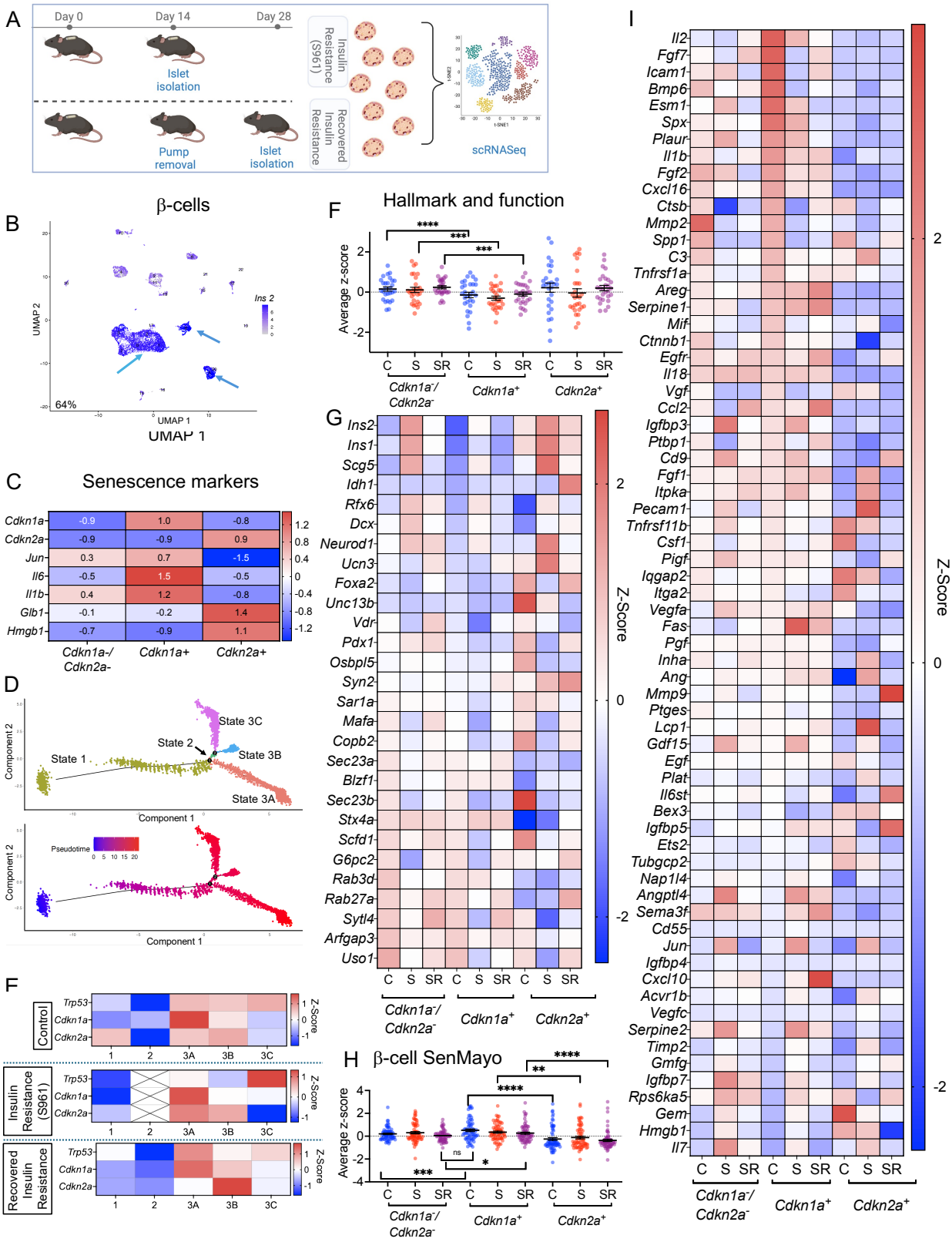
A
Day 0
Day 14
Day 28
Islet isolation
Pump removal
Islet isolation
Insulin Resistance (S961)
Recovered Insulin Resistance
scRNASeq
B
β-cells
Ins 2
UMAP 2
UMAP 1
64%
C
Senescence markers
Cdkn1a
Cdkn2a
Jun
Il6
Il1b
Glb1
Hmgb1
Cdkn1a-/ Cdkn2a-
Cdkn1a+
Cdkn2a+
D
State 3C
State 2
State 1
State 3B
State 3A
Component 2
Component 1
Pseudotime
F
Hallmark and function
Average z-score
C S SR C S SR C S SR
Cdkn1a-/ Cdkn2a-
Cdkn1a+
Cdkn2a+
G
Ins2
Ins1
Scg5
Idh1
Rfx6
Dcx
Neurod1
Ucn3
Foxa2
Unc13b
Vdr
Pdx1
Osbpl5
Syn2
Sar1a
Mafa
Copb2
Sec23a
Blzf1
Sec23b
Stx4a
Scfd1
G6pc2
Rab3d
Rab27a
Sytl4
Arfgap3
Uso1
Z-Score
F
Control
Insulin Resistance (S961)
Recovered Insulin Resistance
Trp53
Cdkn1a
Cdkn2a
1 2 3A 3B 3C
H
β-cell SenMayo
Average z-score
ns
I
Il2
Fgf7
Icam1
Bmp6
Esm1
Spx
Plaur
Il1b
Fgf2
Cxcl16
Ctsb
Mmp2
Spp1
C3
Tnfrsf1a
Areg
Serpine1
Mif
Ctnnb1
Egfr
Il18
Vgf
Ccl2
Igfbp3
Ptbp1
Cd9
Fgf1
Itpka
Pecam1
Tnfrsf11b
Csf1
Pigf
Iqgap2
Itga2
Vegfa
Fas
Pgf
Inha
Ang
Mmp9
Ptges
Lcp1
Gdf15
Egf
Plat
Il6st
Bex3
Igfbp5
Ets2
Tubgcp2
Nap1l4
Angptl4
Sema3f
Cd55
Jun
Igfbp4
Cxcl10
Acvr1b
Vegfc
Serpine2
Timp2
Gmfg
Igfbp7
Rps6ka5
Gem
Hmgb1
Il7
Z-Score

Figure 1. Subpopulations of senescent β-cells with different functional and SASP transcriptional profiles. (A) Reanalysis of scRNASeq data (GSE149984) of islets isolated from C57Bl6/J male mice (7- to 8-month-old retired breeders) under three conditions: control (C), S961-induced insulin resistance for 2 weeks (S) and S961-induced insulin resistance followed by a 2-week recovery period (SR); **(B)** UMAP plot displaying the major islet-cell cluster of mouse β-cells based on *Ins2* expression; **(C)** Heatmap of senescence marker genes with individual z-scores. (**D**) Trajectory analysis scRNASeq from non-senescent to senescent mouse β-cells showing different stages along a pseudo-timecourse and (**E**) specific senescent gene expression per metabolic condition; **(F)** Scatter plots of average z-score expression levels of hallmark and functional genes in each subpopulation; Mean+/- SEM; expression levels analyzed by Wilcoxon matched-pairs signed rank test (F); *p<0.01, **p<0.001, ***p<0.0001 and ****p<0.00001. Data are results from 2939 β-cells in C, 2896 β-cells from S961R conditions and 2513 cells from SR; islets were isolated from four mice per condition as previously published [(1)]. The midpoint of 0 represents average expression across all samples. (**G)** Heatmap of β-cell hallmark and function genes. The graph shows the expression of the genes in three different cell subpopulations of non-senescent β-cells (*Cdkn1a*$^{-}$*/Cdkn2a*$^{-}$) and *Cdkn1a*$^{+}$, *Cdkn2a*$^{+}$ under the three different metabolic conditions described. (H) Scatter plots of average z-score expression levels of b-cell SenMayo score. Mean+/- SEM; expression levels analyzed by Wilcoxon matched-pairs signed rank test; *p<0.01, ***p<0.001 and ****p<0.0001. **(F)** β SenMayo: Heatmap of selected genes related to senescence and SASP in the same three cell subpopulations under the different metabolic conditions.

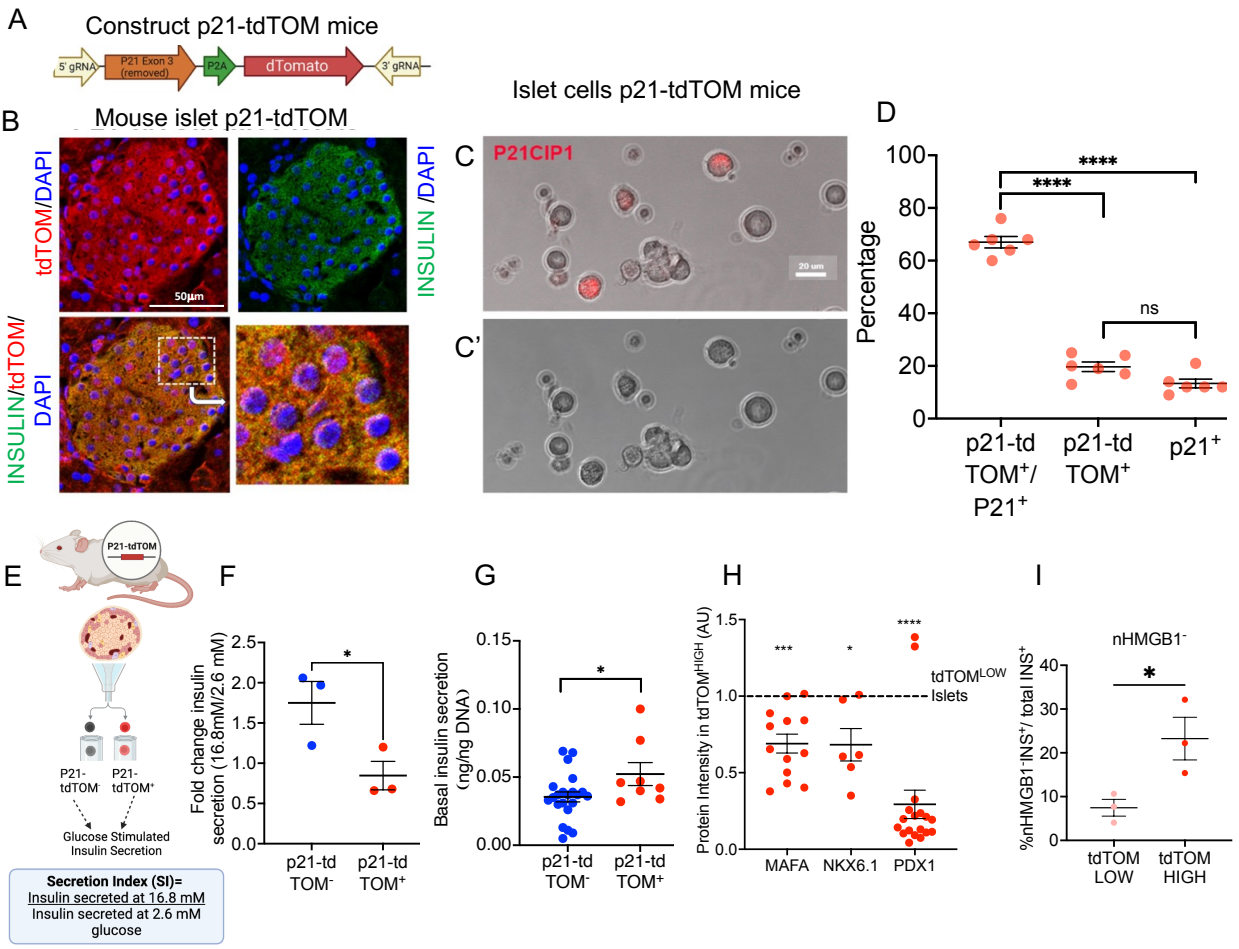
A
Construct p21-tdTOM mice
5' gRNA
P21 Exon 3 (removed)
P2A
dTomato
3' gRNA
B
Mouse islet p21-tdTOM
tdTOM/DAPI
INSULIN /DAPI
INSULIN/tdTOM/ DAPI
50µm
C
Islet cells p21-tdTOM mice
P21CIP1
20 um
C'
D
Percentage
****
****
ns
p21-td TOM+/ P21+
p21-td TOM+
p21+
E
P21-tdTOM
P21- tdTOM-
P21- tdTOM+
Glucose Stimulated Insulin Secretion
Secretion Index (SI)=
Insulin secreted at 16.8 mM
Insulin secreted at 2.6 mM glucose
F
Fold change insulin secretion (16.8mM/2.6 mM)
p21-td TOM-
p21-td TOM+
G
Basal insulin secretion (ng/ng DNA)
p21-td TOM-
p21-td TOM+
H
Protein Intensity in tdTOMHIGH (AU)
tdTOMLOW Islets
MAFA
NKX6.1
PDX1
I
nHMGB1-
%nHMGB1-INS+/ total INS+
tdTOM LOW
tdTOM HIGH
J
MAFA
NKX6.1
PDX1
HMGB1
tdTOM HIGH/DAPI
tdTOM LOW/DAPI
MFI 31.8
MFI 38.1
MFI 73.8
MFI 34.9
MFI 11.7
MFI 16.1
MFI 18.9
MFI 13.7
50 um

Figure 2. The p21^{+}- β-cell subpopulation was dysfunctional and lost its identity. **(A)** P2A-dTomato transgene used in the generation of *p21*-tdTomato mice, inserted at the end of the coding region using CRISPR; **(B)** Panels of different confocal microscopy channels reveal co-expression of insulin and *p21* in islet cells; inset shows its nuclear localization. Representative image shown from n=7 mice; **(C)** Live fluorescence with bright field microscopy of dispersed islets isolated from 3-month-old *p21*-tdTomato, bar 20 µm **(C')** Bright field channel only showing live islet cells; **(D)** The proportion of tdTomato and p21 in islets analyzed by FACS from 6 tdTomato mice (male and female, 40-65 weeks). Each dot represents one mouse. ****p<0.0001, one-way ANOVA. **(E)** Islet isolation, dissociation and sorting based on tdTomato signal to purify P21-tdTOM+ and P21-tdTOM- for functional analysis; **(F)** Secretion Index = Ratio of insulin secreted at 16.8 mM glucose compared to 2.8 mM glucose; n=3 biological replicates; *p<0.05 by two-way paired t-test **(G)** Basal insulin secretion in P21-tdTOM+ and P21-tdTOM- cells separated by flow cytometry; n=2-5 technical replicates from 3 biological replicates. Mean +/- SEM; islets isolated from 4 Male mice (53-70 weeks) and 3 Female mice (51-72 weeks). *p<0.05 by two-way unpaired t-test. **(H)** Loss of β-cell identity at the protein level. Semiquantification of protein intensity in confocal immunofluorescent images from tdTOM^{HIGH} islets respect to tdTOM^{LOW}. Each point represents an individual islet from three P21-tdTOM+ female mice (17-22 weeks). **(I)** HMGB1 nuclear exclusion frequency in INSULIN+ cells in islets from tdTOM^{HIGH} and tdTOM^{LOW}. Each point represents an individual islet from three P21-tdTOM+ female mice (17-22 weeks). **(J)** Representative images of Figure 2H and 2I comparing protein expression of β-cell hallmark genes in islets from tdTOM^{HIGH} and tdTOM^{LOW} . tdTomato (red), β-cell related genes and HMGB1 in green. Mean fluorescence intensity (MFI) for red channel intensity.

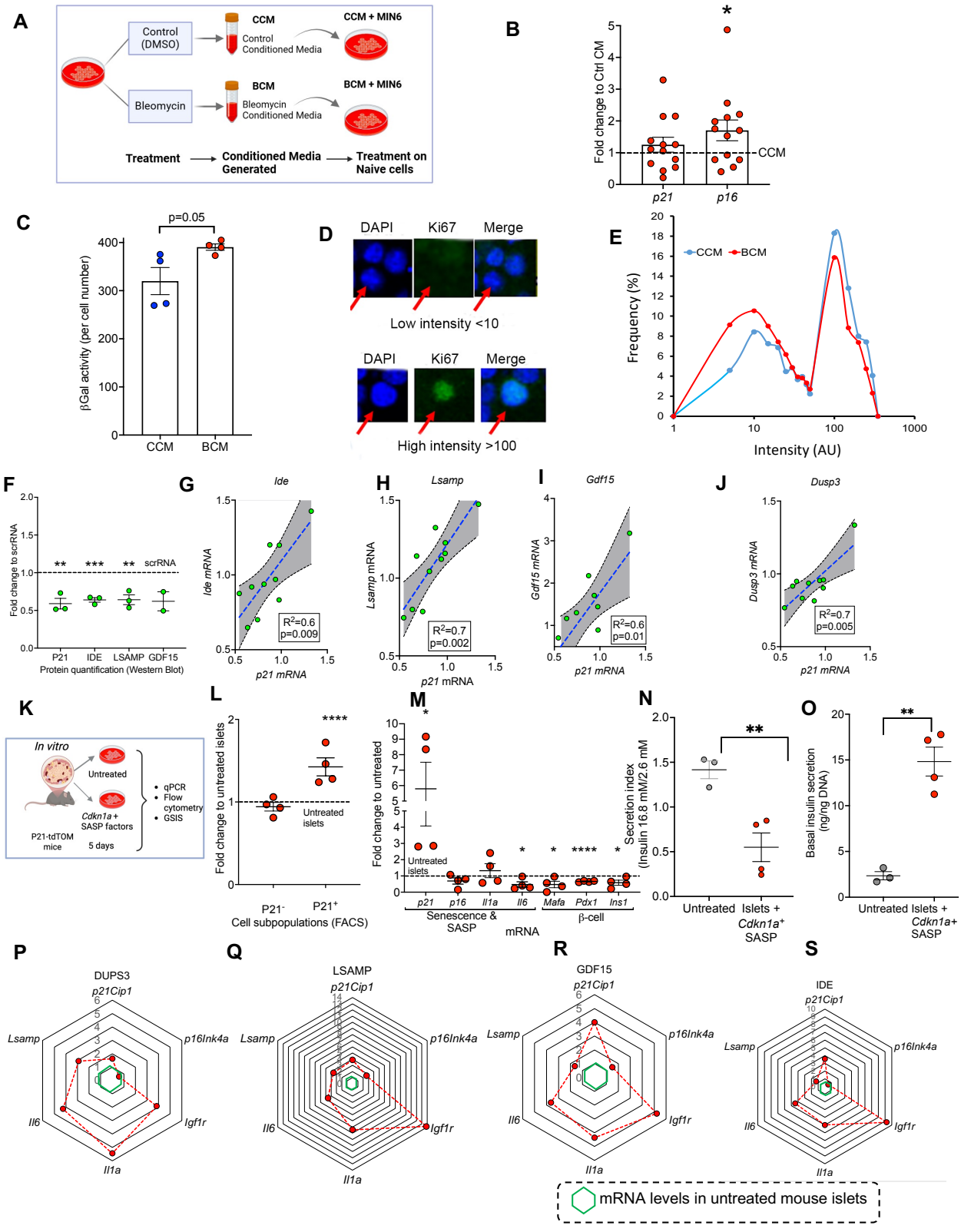
A
Control (DMSO)
Bleomycin
CCM
Control Conditioned Media
CCM + MIN6
BCM
Bleomycin Conditioned Media
BCM + MIN6
Treatment
Conditioned Media Generated
Treatment on Naive cells
B
Fold change to Ctrl CM
CCM
p21
p16
C
p=0.05
βGal activity (per cell number)
CCM
BCM
D
DAPI
Ki67
Merge
Low intensity <10
High intensity >100
E
CCM
BCM
Frequency (%)
Intensity (AU)
F
Fold change to scrRNA
scrRNA
P21
IDE
LSAMP
GDF15
Protein quantification (Western Blot)
G
Ide
Ide mRNA
p21 mRNA
R²=0.6
p=0.009
H
Lsamp
Lsamp mRNA
p21 mRNA
R²=0.7
p=0.002
I
Gdf15
Gdf15 mRNA
p21 mRNA
R²=0.6
p=0.01
J
Dusp3
Dusp3 mRNA
p21 mRNA
R²=0.7
p=0.005
K
In vitro
Untreated
Cdkn1a+ SASP factors
P21-tdTOM mice
5 days
qPCR
Flow cytometry
GSIS
L
Fold change to untreated islets
Untreated islets
P21⁻
P21⁺
Cell subpopulations (FACS)
M
Fold change to untreated
Untreated islets
p21
p16
Il1a
Il6
Mafa
Pdx1
Ins1
Senescence & SASP
β-cell
mRNA
N
Secretion index (Insulin 16.8 mM/2.6 mM)
Untreated
Islets + Cdkn1a⁺ SASP
O
Basal insulin secretion (ng/ng DNA)
Untreated
Islets + Cdkn1a+ SASP
P
DUPS3
p21Cip1
p16Ink4a
Igf1r
Il1a
Il6
Lsamp
Q
LSAMP
R
GDF15
S
IDE
mRNA levels in untreated mouse islets

Figure 3. Secondary senescence: β-cell SASP has non-cell autonomous effects on neighboring cells. **(A)** Workflow to test the effects of SASP on naïve MIN6 cells. **(B)** Effects of BCM on *p21* and *p16* mRNA expression of naïve MIN6 cells (n=13-14 technical replicates from 3 biological replicates*) *p<0.05*, analyzed by non-parametric Wilcoxon test; **(C)** β-Gal^{+} activity normalized per cell number (n=4 biological replicates); **(D)** Cumulative frequency graph of Ki67 staining of MIN6 cells reflecting proliferating subpopulations (Cells counted: n=2911 for CCM, n=3000 for BCM (4 two technical replicates from 2 biological replicates); **(E)** Protein quantification by Western Blot of selected *Cdkn1a*+ SASP factors after treatment with p21 siRNA at 50 nM in MIN6 cells (n=3 biological replicates). Mean +/- SEM **p<0.005 and ***p<0.0005; **(F-I**) Expression levels of *Cdkn1a*-SASP factors from individual samples and their correlations with *Cdkn1a* expression. Lines of best fit are shown, along with dotted lines indicating 95% confidence intervals. p-values were calculated using the null hypothesis that the slope of the best fit line equals 0; **(J)** Treatment of islets from p21-tdTom mice with *Cdkn1a* SASP factors (LSAMP+DUSP3+GDF15+IDE) during 5 days (female and male, 12-20 weeks old); **(K)** Cellular subpopulations as determined by flow cytometry of dispersed islets after treatment; **(L)** Effects of *Cdkn1a*+ SASP factors on transcription of selected senescence and key β-cell genes; **(M)** Secretion index of islets treated with *Cdkn1a*+ SASP factors; **(N)** Basal insulin secretion (n=4 biological replicates). Mean+/- SEM; expression levels analyzed by two-way t-tests; *p<0.01, **p<0.001 ***p<0.0001 and ****p<0.00001. **(O-R)** Radar plots of qPCR results for the mean expression of senescence and SASP genes. MIN6 cells treated with an individual SASP. Mean+/- SEM; n= 2 biological replicates with 2-3 technical replicates each. Concentrations of SASP proteins used in culture media are shown in **Table 1**. Mean+/- SEM; expression levels analyzed by two-way t-tests; *p<0.01, **p<0.001 ***p<0.0001 and ****p<0.00001.

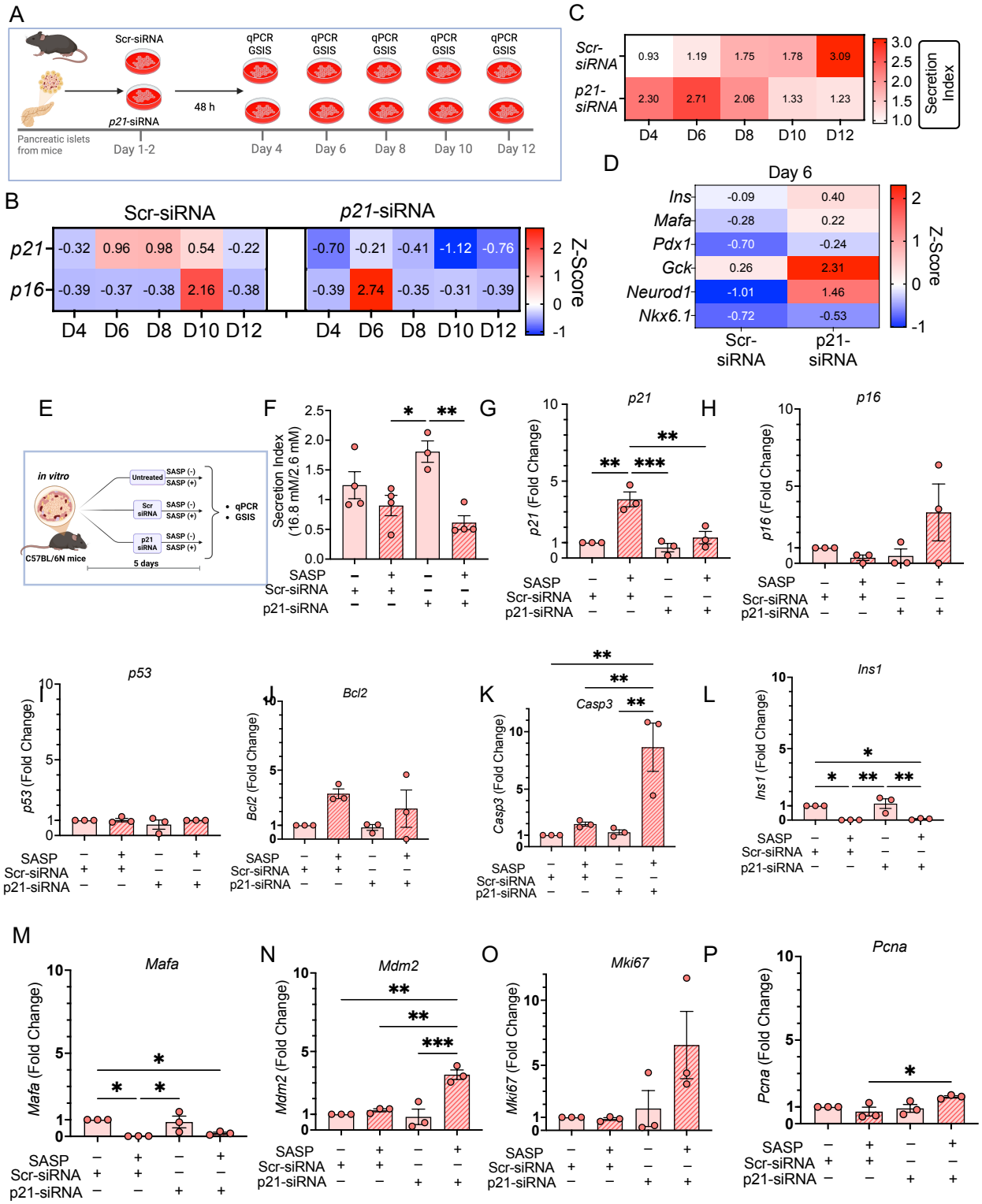
A
Scr-siRNA
p21-siRNA
48 h
qPCR
GSIS
Pancreatic islets from mice
Day 1-2
Day 4
Day 6
Day 8
Day 10
Day 12
B
Scr-siRNA
p21-siRNA
p21
p16
-0.32 0.96 0.98 0.54 -0.22
-0.39 -0.37 -0.38 2.16 -0.38
-0.70 -0.21 -0.41 -1.12 -0.76
-0.39 2.74 -0.35 -0.31 -0.39
D4 D6 D8 D10 D12
Z-Score
C
Scr-siRNA
p21-siRNA
0.93 1.19 1.75 1.78 3.09
2.30 2.71 2.06 1.33 1.23
Secretion Index
D
Day 6
Ins
Mafa
Pdx1
Gck
Neurod1
Nkx6.1
-0.09 0.40
-0.28 0.22
-0.70 -0.24
0.26 2.31
-1.01 1.46
-0.72 -0.53
Scr-siRNA
p21-siRNA
Z-Score
E
in vitro
Untreated
Scr siRNA
p21 siRNA
SASP (-)
SASP (+)
• qPCR
• GSIS
C57BL/6N mice
5 days
F
Secretion Index (16.8 mM/2.6 mM)
G
p21
p21 (Fold Change)
H
p16
p16 (Fold Change)
SASP
Scr-siRNA
p21-siRNA
I
p53
p53 (Fold Change)
J
Bcl2
Bcl2 (Fold Change)
K
Casp3
Casp3 (Fold Change)
L
Ins1
Ins1 (Fold Change)
M
Mafa
Mafa (Fold Change)
N
Mdm2
Mdm2 (Fold Change)
O
Mki67
Mki67 (Fold Change)
P
Pcna
Pcna (Fold Change)

Figure 4. *Cdkn1a*$^{+}$ SASP factors induce secondary cellular senescence in mouse pancreatic islets *in vitro*. (A) Experimental design of the conditional *p21* knock down timecourse on mouse islets to assess effects on transcription and function. **(B)** Timecourse expression levels of *p21* and *p16* mRNA under control (Scr-siRNA) and conditional p21 knock down (p21-SiRNA, 50nM); **(C)** Timecourse of β-cell function as reflected by secretion index at different days after conditional knockdown of *p21*; **(D)** β-cell hallmark and function genes after *p21* conditional knockdown (p21-siRNA) at day 6. 100 islets per condition from retired male breeders n = 7 biological replicates**;** data shown as heatmap of z-score for panels B, D and of secretion index for C. (**E**) Experimental design for the evaluation of *p21*-SASP factors after *p21* conditional knockdown (p21-siRNA) in mouse islets (**F**) Secretion index from static GSIS from *p21*-siRNA or *Scr*-siRNA with/without SASP factors (LSAMP+DUSP3+GDF15+IDE) during 5 days. Islets from 33 male C57Bl/N mice were used (6-9 months). (**G-P**) Transcriptomic gene levels from same experiment design using islets from 24 female and male C57Bl/N mice (17 weeks to 9 months). Mean+/-SEM, One-way ANOVA, *p<0.05, **p<0.01, ***p<0.001, ****p<0.0001.

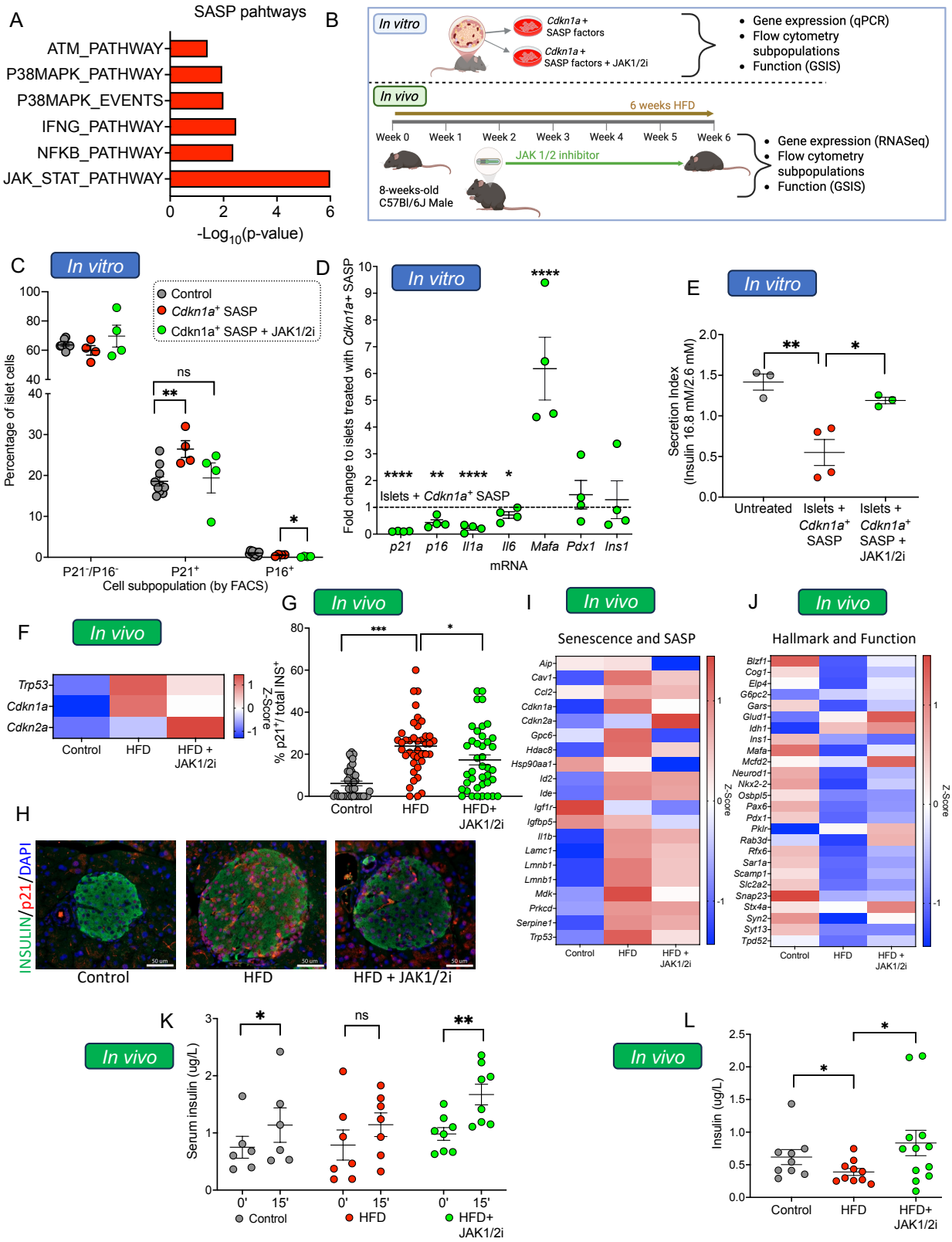
A
SASP pahtways
ATM_PATHWAY
P38MAPK_PATHWAY
P38MAPK_EVENTS
IFNG_PATHWAY
NFKB_PATHWAY
JAK_STAT_PATHWAY
-Log10(p-value)
B
In vitro
Cdkn1a+ SASP factors
Cdkn1a+ SASP factors + JAK1/2i
Gene expression (qPCR)
Flow cytometry subpopulations
Function (GSIS)
In vivo
6 weeks HFD
Week 0
Week 1
Week 2
Week 3
Week 4
Week 5
Week 6
JAK 1/2 inhibitor
8-weeks-old C57Bl/6J Male
Gene expression (RNASeq)
Flow cytometry subpopulations
Function (GSIS)
C
In vitro
Control
Cdkn1a+ SASP
Cdkn1a+ SASP + JAK1/2i
Percentage of islet cells
ns
**
*
P21-/P16-
P21+
P16+
Cell subpopulation (by FACS)
D
In vitro
Fold change to islets treated with Cdkn1a+ SASP
Islets + Cdkn1a+ SASP
p21
p16
Il1a
Il6
Mafa
Pdx1
Ins1
mRNA
E
In vitro
Secretion Index (Insulin 16.8 mM/2.6 mM)
Untreated
Islets + Cdkn1a+ SASP
Islets + Cdkn1a+ SASP + JAK1/2i
F
In vivo
Trp53
Cdkn1a
Cdkn2a
Control
HFD
HFD + JAK1/2i
Z-score
G
In vivo
% p21+/ total INS+
Control
HFD
HFD+ JAK1/2i
H
INSULIN/p21/DAPI
Control
HFD
HFD + JAK1/2i
I
In vivo
Senescence and SASP
Aip
Cav1
Ccl2
Cdkn1a
Cdkn2a
Gpc6
Hdac8
Hsp90aa1
Id2
Ide
Igf1r
Igfbp5
Il1b
Lamc1
Lmnb1
Lmnb1
Mdk
Prkcd
Serpine1
Trp53
Z-Score
J
In vivo
Hallmark and Function
Blzf1
Cog1
Elp4
G6pc2
Gars
Glud1
Idh1
Ins1
Mafa
Mcfd2
Neurod1
Nkx2-2
Osbpl5
Pax6
Pdx1
Pklr
Rab3d
Rfx6
Sar1a
Scamp1
Slc2a2
Snap23
Stx4a
Syn2
Syt13
Tpd52
Z-Score
K
In vivo
Serum insulin (ug/L)
0'
15'
Control
HFD
HFD+ JAK1/2i
L
In vivo
Insulin (ug/L)
Control
HFD
HFD+ JAK1/2i

Figure 5. Secondary senescence induced by *Cdkn1a*+ SASP factors is counteracted by JAK1/2 inhibitors (JAK1//2i) in mouse islets *in vitro* and *in vivo*. **(A)** Pathway analysis of SASP-regulating pathways in RNA-seq data from mouse senescent β-cells (6) reveals upregulation of the JAK/STAT pathway. **(B**) Experimental design ***In vitro:*** Treatment of islets from p21-tdTom mice with *Cdkn1a* SASP factors (LSAMP+DUSP3+GDF15+IDE) in combination with JAK1/2 inhibitor (JAK1/2i). ***In vivo:*** male C57Bl/6N mice were fed a high-fat diet (HFD) for 6 weeks and treated for 4 weeks with JAK1/2i. n=9 control, n=11 HFD group, n=13 HFD + JAK1/2i; **(C)** Flow cytometry analysis of dispersed islets treated with *Cdkn1a* SASP factors with or without JAK1/2i; **(D)** Transcriptional analysis of islets treated with *Cdkn1a* SASP factors with or without JAK1/2i; **(E)** Functional analysis of islets treated with *Cdkn1a* SASP factors with or without JAK1/2i. n=4 independent experiments. Mean+/- SEM; expression levels analyzed by two-way t-tests respect to control; *p<0.01, **p<0.001 ***p<0.0001 and ****p<0.00001. **(F)** Heatmap showing expression of key senescent genes in islets isolated from different treated groups; **(G)** Percentage of p21 (red) positive cells in INSULIN (green) positive cells determined by semiquantitative immunohistochemistry in 3 groups; Control, HFD, and HFD+JAK1/2i. Four 16-24 weeks of female p21-tdTom mice were used in each group, and 933-1245 islets were counted/group. **(H)** Representative images of islets immunostained for p21 (red) positive cells in INSULIN (green) in different treatment groups. Scale bar 50 μm. **(I)** Z-score expression of senescence and SASP genes; **(J)** Z-score expression of β-cell hallmark and functional genes. **(K)** GSIS by sampling plasma at minutes 0 and 15 during IPGTT. Mean +/- SEM; *p<0.01, **p<0.001 two-way paired t-test **(L)** Fed plasma insulin in mice. Mean +/- SEM; *p<0.01, **p<0.001 by two-way unpaired t-test.

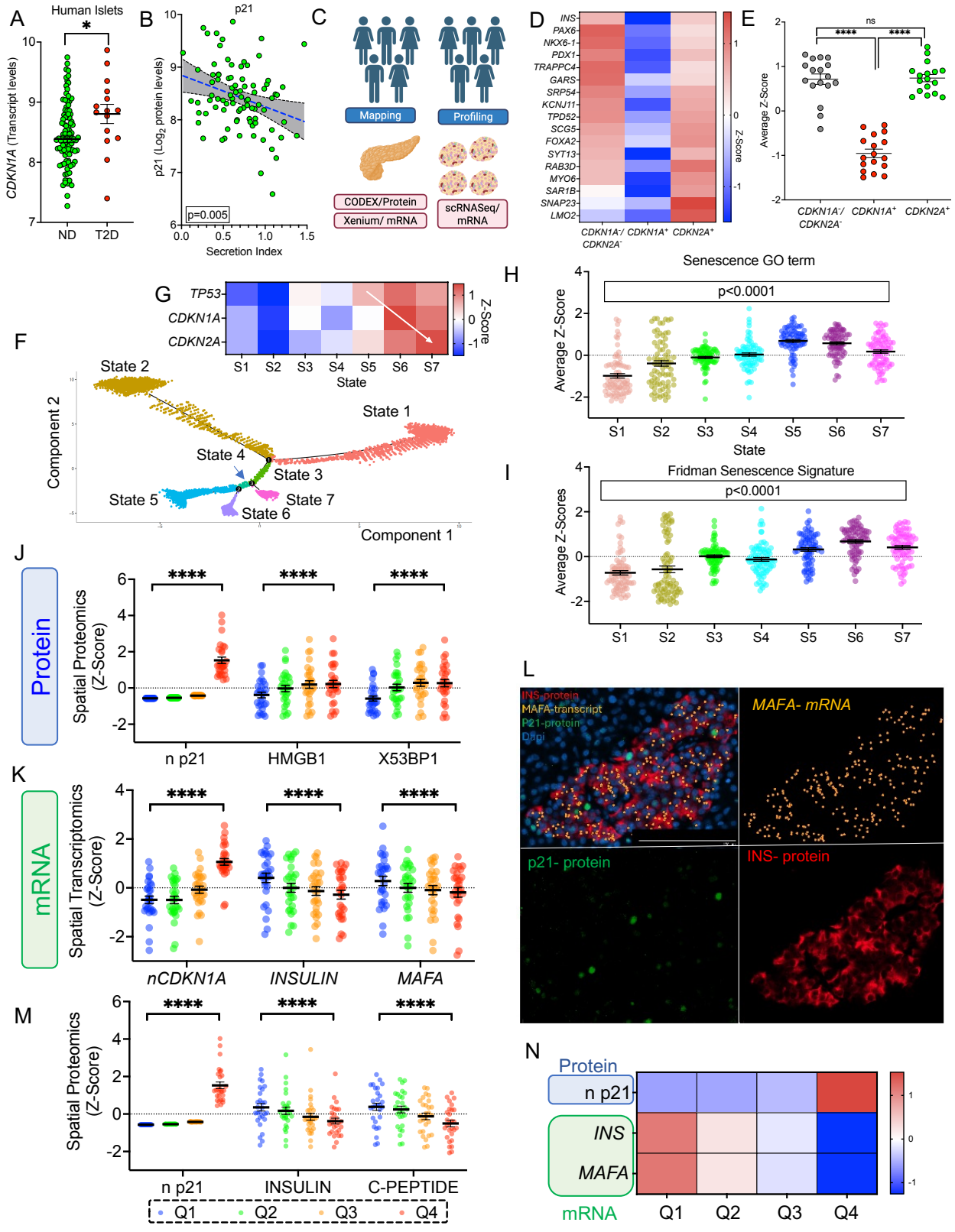
A
Human Islets
CDKN1A (Transcript levels)
ND
T2D
B
p21
p21 (Log2 protein levels)
Secretion Index
p=0.005
C
Mapping
Profiling
CODEX/Protein
Xenium/ mRNA
scRNASeq/ mRNA
D
INS
PAX6
NKX6-1
PDX1
TRAPPC4
GARS
SRP54
KCNJ11
TPD52
SCG5
FOXA2
SYT13
RAB3D
MYO6
SAR1B
SNAP23
LMO2
CDKN1A-/ CDKN2A-
CDKN1A+
CDKN2A+
Z-Score
E
ns
Average Z-Score
F
State 2
State 1
State 4
State 3
State 5
State 7
State 6
Component 1
Component 2
G
TP53
CDKN1A
CDKN2A
Z-Score
State
H
Senescence GO term
p<0.0001
Average Z-Score
I
Fridman Senescence Signature
p<0.0001
Average Z-Scores
J
Protein
Spatial Proteomics (Z-Score)
n p21
HMGB1
X53BP1
K
mRNA
Spatial Transcriptomics (Z-Score)
nCDKN1A
INSULIN
MAFA
L
INS-protein
MAFA-transcript
P21-protein
Dapi
MAFA- mRNA
p21- protein
INS- protein
M
Spatial Proteomics (Z-Score)
n p21
INSULIN
C-PEPTIDE
Q1
Q2
Q3
Q4
N
Protein
n p21
INS
MAFA
mRNA
Q1
Q2
Q3
Q4

Figure 6. Loss of function and identity in human p21^{+} β-cells. (A) *CDKN1A* mRNA levels in islets from human donors without (ND) and with Type 2 Diabetes (T2D); **(B)** Linear correlation between p21 protein levels in human islets and their function as expressed by the secretion index; **(C)** KAPPSen study design aimed at mapping and profiling senescent cells in both whole and dispersed human pancreas; **(D-E)** Heatmap and dot plot of human β-cell scRNASeq data for selected β-cell functional genes across three cell subpopulations: non-senescent β-cells (*CDKN1A*$^{-}$*/CDKN2A*$^{-}$), *CDKN1A*$^{+,}$ and *CDKN2A*$^{+}$*;* **(F)** Pseudotime trajectory analysis of scRNASeq from non-senescent to senescent human β-cells; **(G)** Heatmap showing expression levels of key senescence genes at various stages during the senescence trajectory; **(H)** scRNASeq expression levels of genes in the senescence Gene Ontology (GO) category and **(I)** Fridman gene senescent scores. Data shows individual cells in each trajectory state, mean ± SEM; expression levels analyzed via 2-way ANOVA. Quartiles of nuclear P21 protein expression derived from spatial proteomic (CODEX) data, only from β-cells. **(J)** Co-expression of senescence proteins within cells exhibiting quartile distribution of nuclear P21. **(K)** Co-expression of β-cell transcripts within cells exhibiting quartile distribution of nuclear P21. **(L)** Representative image of integrated CODEX (INSULIN (red) and p21 (green) protein) with Xenium (*MAFA* (orange) transcript). **(M)** Quartiles of nuclear *CDKN1A* mRNA expression from Xenium and co-expression with hallmark β-cell genes. **(N)** Heatmap showing overlapping co-expression of nuclear P21 with β-cell hallmark genes.

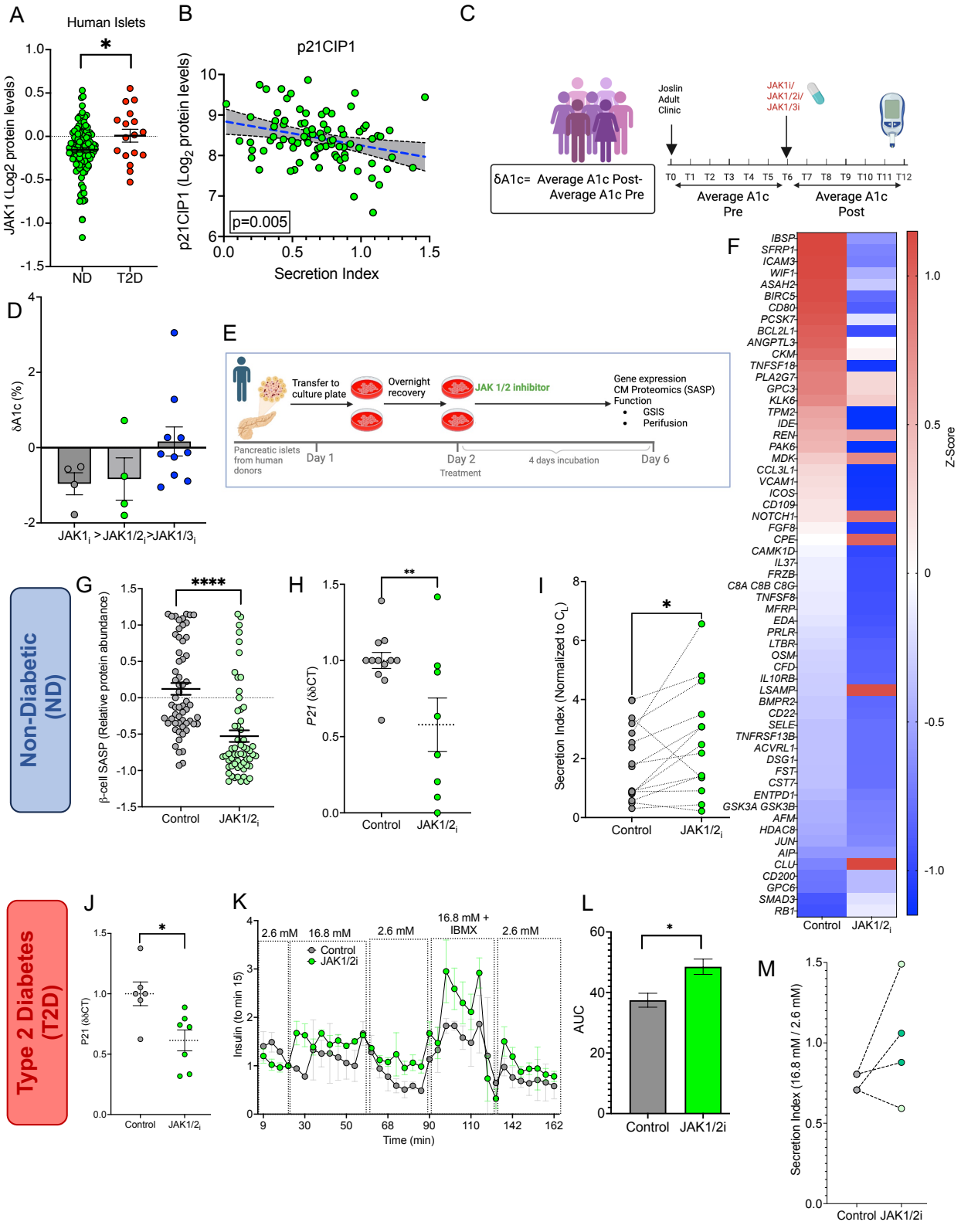
A
Human Islets
JAK1 (Log2 protein levels)
ND
T2D
B
p21CIP1
p21CIP1 (Log2 protein levels)
p=0.005
Secretion Index
C
Joslin Adult Clinic
JAK1i/ JAK1/2i/ JAK1/3i
δA1c= Average A1c Post- Average A1c Pre
T0 T1 T2 T3 T4 T5 T6 T7 T8 T9 T10 T11 T12
Average A1c Pre
Average A1c Post
D
δA1c (%)
JAK1i > JAK1/2i > JAK1/3i
E
Transfer to culture plate
Overnight recovery
JAK 1/2 inhibitor
Gene expression
CM Proteomics (SASP)
Function
GSIS
Perifusion
Pancreatic islets from human donors
Day 1
Day 2
Treatment
4 days incubation
Day 6
F
IBSP
SFRP1
ICAM3
WIF1
ASAH2
BIRC5
CD80
PCSK7
BCL2L1
ANGPTL3
CKM
TNFSF18
PLA2G7
GPC3
KLK6
TPM2
IDE
REN
PAK6
MDK
CCL3L1
VCAM1
ICOS
CD109
NOTCH1
FGF8
CPE
CAMK1D
IL37
FRZB
C8A C8B C8G
TNFSF8
MFRP
EDA
PRLR
LTBR
OSM
CFD
IL10RB
LSAMP
BMPR2
CD22
SELE
TNFRSF13B
ACVRL1
DSG1
FST
CST7
ENTPD1
GSK3A GSK3B
AFM
HDAC8
JUN
AIP
CLU
CD200
GPC6
SMAD3
RB1
Control
JAK1/2i
Z-Score
Non-Diabetic (ND)
G
β-cell SASP (Relative protein abundance)
Control
JAK1/2i
H
P21 (δδCT)
Control
JAK1/2i
I
Secretion Index (Normalized to CL)
Control
JAK1/2i
Type 2 Diabetes (T2D)
J
P21 (δδCT)
Control
JAK1/2i
K
2.6 mM
16.8 mM
2.6 mM
16.8 mM + IBMX
2.6 mM
Control
JAK1/2i
Insulin (to min 15)
Time (min)
L
AUC
Control
JAK1/2i
M
Secretion Index (16.8 mM / 2.6 mM)
Control
JAK1/2i

1088

1089

Figure 7. Effects of JAK1/2i on secretion of human β-cell function. (A) JAK1 protein levels in human islets from non-diabetics (ND) and Type 2 diabetes (T2D) donors**; (B)** linear regression of JAK1 protein levels and secretion index from human islets; **(C)** Analysis of data from Joslin Diabetes Center's adult clinic. Longitudinal glycated hemoglobin (A1c) levels from Individuals with T2D and who had been prescribed JAK inhibitors for medical indications independent from diabetes. The effect of the JAK inhibitors treatment was measured by the change of A1c. δA1c = (Average A1c Post) – (Average A1c Pre) **(D)** Mean A1c change before and after starting treatment with a specified JAK inhibitor in people with Type 2 Diabetes. **(E)** Workflow of human islets from ND and T2D donors treated with JAK1/2i or JAK1/3i for 4 days. **(F-G)** Heatmap and dotplot of SASP (log_2-protein abundance) secretion in conditioned media collected from human untreated (control) or treated (JAK1/2i). Top upregulated human β-cell SASP proteins were selected. Paired analysis per analyte was performed between conditions. Cell numbers varied from one donor to another but were maintained constant across treatments. Donor 1- 526,000 cells/treatment; donor 2-192,000 cells/treatment; donor 3- 231,000 cells/treatment; donors 4&5- 87,500 cells/treatment. **(H)** *p21* mRNA levels in human islets from ND donors. **(I)** β-cell function evaluated by GSIS in human islets from ND donors with 1-3 replicates per donor. **(J)** Effects of JAK1/2i in *p21* mRNA in islets from T2D donors; **(K)** β-cell function evaluated with islet perifusion in islets from two donors with T2D, BMI 38.3 and 42.2, age 58 and 55 years old, respectively. **(L)** Static GSIS from two T2D female donors using JAK1/2i (momelotinib: dark green, and baricitinib: light green), both BMI 42.2, age 49 and 55 years old.

Table 1. Selected SASP factors and their role according to senescence cell subpopulation

Factor	Name	Subpopulation	Concentration in plasma and used in culture	Role in senescence or T2D	Ref
LSAMP	Limbic system associated membrane protein	*Cdkn1a*$^{+}$	150 µg/L	β-cell function and insulin resistance	(33)
IDE	Insulin degrading enzyme	*Cdkn1a*$^{+}$	0.31 µg/L	Impaired insulin secretion	(34, 35)
DUSP3	Dual specificity phosphatase 3	*Cdkn1a*$^{+}$	1.3 µg/L	Cell proliferation and DDR	(36-38)
GDF15	Growth differentiation factor 15	*Cdkn1a*$^{+}$	1.3 µg/L	SASP, mitochondrial dysfunction	(39-44)

For the DDR-DNA damage response, plasma concentrations were taken from the Human Protein Atlas and determined by immunoassay (https://www.proteinatlas.org).